Food Chemistry 394 (2022) 133410

Contents lists available at ScienceDirect

Food Chemistry

journal homepage: www.elsevier.com/locate/foodchem

Influence of food macrostructure on the kinetics of acidification in the pig stomach after the consumption of rice- and wheat-based foods: Implications for starch hydrolysis and starch emptying rate

Joanna Nadia [a,b], Alexander G. Olenskyj [c], Parthasarathi Subramanian [a], Suzanne Hodgkinson [a], Natascha Stroebinger [a], Talia G. Estevez [c], R. Paul Singh [a,c], Harjinder Singh [a], Gail M. Bornhorst [a,c,*]

[a] Riddet Institute, Massey University, Private Bag 11222, Palmerston North, New Zealand
[b] School of Food and Advanced Technology, Massey University, Private Bag 11222, Palmerston North, New Zealand
[c] Department of Biological and Agricultural Engineering, University of California, Davis, CA 95618, USA

ARTICLE INFO

Keywords:
Food structure
Gastric digestion
Amylase activity
Starch hydrolysis
Gastric acidification

ABSTRACT

How the stomach can serve as a biochemical environment for starch digestion and the implications on starch emptying are not well-understood. Biochemical changes during gastric digestion of cooked wheat- and rice-based diets of varying particle size and microstructure were investigated using a growing pig model. In larger-particle size diets (rice grain, rice noodle, pasta), pH >3 was maintained in the proximal stomach digesta even until 240 min digestion, resulting in extended remaining amylase activity and accumulation of maltose from starch hydrolysis in the stomach. In smaller-particle size diets (couscous, rice couscous, semolina porridge), gastric acidification occurred faster to produce homogeneous intragastric pH and deactivated amylase. The hypothesis of the study was that food macrostructure would impact gastric acidification kinetics, and the resulting biochemical environment for starch hydrolysis in the stomach may further affect the mechanisms of food breakdown in the stomach and gastric emptying of starch.

1. Introduction

During gastrointestinal digestion, starch in food is converted to oligosaccharides by salivary amylase and pancreatic amylase, producing maltose, maltotriose, and limit dextrins as the end products. These oligosaccharides are hydrolyzed further by the brush border enzymes in the small intestine to produce glucose, which is absorbed into the bloodstream (Holmes, 1971). Hydrolysis of starch in food has been associated mainly with the action of pancreatic amylase during small intestinal digestion. In contrast, the contribution of salivary amylase during mastication on starch hydrolysis is less well-understood, as mastication only lasts for <5 to 90 s. Gastric digestion occurs between mastication and intestinal digestion (typically from 0–4 h) and has not been commonly considered as a location for starch hydrolysis due to the low pH of gastric secretions (Nadia, Bronlund, Singh, Singh, & Bornhorst, 2021). However, a number of *in vitro* studies using a gastric digestion system with dynamic pH profile reported hydrolysis of 30–80% starch in food matrices during gastric digestion (Freitas, Boué, et al., 2022; Freitas & Le Feunteun, 2018, 2019; Martens, Bruininx, Gerrits, & Schols, 2020; Nadia, Bronlund, Singh, Singh, & Bornhorst, 2022), suggesting that salivary amylase can remain active during gastric digestion. Remaining amylase activity in the stomach may increase the degree of starch hydrolysis of materials that are emptied to the small intestine, which may increase glucose production in the small intestine and absorption into the blood stream. This hypothesis is supported by a study in which it was reported that lowering the pH of starch-rich foods by consuming an acidic beverage could lower glycemic response in humans, which could be attributed by an early inhibition of salivary amylase during gastric digestion (Freitas, Boué, Benallaoua, Airinei, Benamouzig, & Le Feunteun, 2021; Freitas et al., 2022).

Although the contribution of salivary amylase activity in the stomach to the digestion of starch has been suggested in previous studies, the underlying mechanisms and contributing factors have not been fully elucidated. Slow mixing between acidic gastric secretions with the

* Corresponding author.
E-mail address: gbornhorst@ucdavis.edu (G.M. Bornhorst).

https://doi.org/10.1016/j.foodchem.2022.133410
Received 18 June 2021; Received in revised form 30 May 2022; Accepted 4 June 2022
Available online 7 June 2022

ingested food bolus (i.e., gastric mixing) has been suggested as a possible mechanism describing how the stomach could be a suitable location for remaining salivary amylase activity as long as the pH within the bolus is maintained at pH >3.0 (Bornhorst, 2017; Brownlee, Gill, Wilcox, Pearson, & Chater, 2018). Previous studies have suggested that the gastric mixing process is affected by the buffering capacity and viscosity of the meal (Bornhorst, Rutherfurd, Roman, Burri, Moughan, & Singh, 2014; Freitas & Le Feunteun, 2019; Freitas, Le Feunteun, Panouille, & Souchon, 2018), indicating the potential contribution of food structure to remaining salivary amylase action in a starch-based meal. Nevertheless, there has not been a clear link established between food structure, remaining salivary amylase activity in the stomach, and resulting starch hydrolysis.

The present study determined *in vivo* biochemical changes during gastric digestion in starch from various rice and wheat-based foods, which are dominant global cereal grain sources (Shewry, 2008). This work was focused specifically on the gastric digestion stage, as the role of the stomach in starch digestion is often underestimated and therefore is less investigated. Intestinal digestion-related aspects are outside the scope of the current study, and will be presented elsewhere. It was previously demonstrated in a growing pig model that physical breakdown during gastric digestion of rice- and wheat-based diets of varying macrostructures impacted the dry matter gastric emptying (Nadia, Olenskyj, et al., 2021). Different breakdown rates in the proximal and distal stomach regions for different diets were hypothesized to be affected by initial macrostructures of the diets, leading to different extent of mixing between gastric secretions with the ingested diets. However, it is important to understand how these different physical breakdown rates and gastric mixing processes are related to biochemical modification of the digesta, because biochemical changes by enzymatic activity may cause additional breakdown during digestion, as reported in an *in vitro* system (Nadia et al., 2022). Moreover, biochemical modification of the gastric digesta may affect the properties of the emptied particles (starch hydrolysis and size of emptied particles in the context of this work), and potentially affect digestion in the small intestine and glycemic response profile of the diets (Freitas, Souchon, & Le Feunteun, 2022). Therefore, apparent amylase activity, reducing sugar and free amino group concentrations (as measures of starch and protein hydrolysis, respectively), and the particle size of the suspended solid fraction in gastric digesta were quantified in the current study. Gastric mixing was qualitatively observed through intragastric pH measurement. It was hypothesized that slower gastric mixing would lead to a longer period of high pH in the proximal stomach, allowing salivary amylase to continue hydrolyzing starch until the proximal stomach content was acidified by gastric secretions, which may further affect the structural breakdown during gastric digestion and gastric emptying mechanisms of solid particles. This work was the first to investigate the link between solid starch-based food structure, gastric acidification kinetics due to the food structure, and the resulting biochemical digestion in an *in vivo* system, which provides an understanding on the impact of food structure on biochemical breakdown of starch in food matrix during gastric digestion. The knowledge will be beneficial for the development of starch-based foods with controlled gastric breakdown and starch gastric emptying properties for glycemic response management.

2. Materials & methods

2.1. Experimental diets preparation and characterization

Six experimental diets of three physical structures (grain, couscous, noodle) from two starch sources (Durum wheat and white rice) were investigated. The rice-based diets are referred to as rice grain, rice couscous, rice noodle; the wheat-based diets are referred to as semolina, couscous, and pasta. All diets, except rice couscous, were purchased from Davis Trading, Palmerston North, NZ. The rice couscous manufacturing process, as well as the cooking methods of the experimental diets prior to feeding to the pigs are described in Nadia, Olenskyj, et al. (2021). The diets were prepared separately as basal and test diets (Table S1). Physico-chemical properties of the experimental diets were determined as described in Nadia, Olenskyj, et al. (2021).

2.2. Animal housing and treatment

All protocols in this study were conducted as previously described (Nadia, Olenskyj, et al., 2021), under the approval of the Animal Ethics Committee, Massey University, New Zealand (Protocol 18/128). The study involved 147 entire male growing pigs, which were housed at the research facility in seven separate batches. The pigs were randomly allotted to one of 24 treatment groups (six experimental diets × four digestion time points) to allow for five to six pigs per treatment. Pigs were transitioned from commercial pig feed to their assigned experimental diets within three days (Table S1). During the acclimatization period (at least five days), the pigs were given 20–30 min to eat their meals. At least 18 h prior to sampling time, 70% of sampling day food amount was fed. On the sampling day, a standardized amount (250 g starch equivalent, dry basis) of experimental diet was mixed carefully with TiO_2 (0.5% of the dry weight of the diet) as an indigestible marker prior to feeding. After 30 min of feeding, any uneaten meal was removed and weighed.

2.3. Gastric digesta collection procedure

On sampling day, pigs were anesthetized 30, 60, 120, or 240 min (depending on the assigned digestion time) after consumption of the test diet through intramuscular injection in the neck, as previously described (Nadia, Olenskyj, et al., 2021). Pigs were euthanized 20 min later by an intracardial injection of a lethal dose of pentobarbitone (0.3 mL/kg BW, Pentobarb 300).

For each pig, the gastrointestinal tract was carefully taken out following euthanasia. The stomach was removed, then its esophageal and duodenal ends were clamped. After cleaning with water and drying with absorbent paper, the stomach was laid horizontally on a sampling tray. The stomach was dissected laterally with a single cut from the middle proximal to the middle distal region, then the cut outer muscles were clamped and moved to the side. Intragastric pH was immediately measured at 10 locations around the stomach (Fig. 1A) with a pH meter (PL-700 PV Bench Top Meter, GonDo, Taipei, Taiwan), following Bornhorst et al. (2014). At each location, pH was measured under the gastric tissue at approximately the center height of the digesta. Average pH values from each diet × time × measurement location were used to generate intragastric pH maps using the "jet" color map in Matlab. pH between measurement locations was interpolated with linear interpolation method using a surface plot function.

Gastric digesta from the proximal and distal gastric regions was weighed and mixed carefully to achieve uniform pH. Subsequently, a 10–15 g subsample from each stomach region was taken and immediately frozen on dry ice for amylase activity analysis. The pH of the mixed sample from each stomach region was measured, then the pH of the rest of the gastric contents was adjusted to pH 8–10 by careful mixing with <1 mL 50%-w/w NaOH solution to inactivate digestive enzymes. The pH-adjusted digesta was distributed to containers for particle size measurement (fresh sample) and the remaining sample was frozen for chemical and microstructural analysis (frozen or freeze-dried sample) (Fig. 1A).

2.4. Gastric digesta chemical analysis

2.4.1. Reducing sugar and free amino groups

The pH-adjusted, frozen samples (~7 g) were thawed at 37 °C for 1 h, transferred to pre-weighed tubes, and centrifuged (4,122 × *g*, 20 min) to separate the digesta into three fractions: solid, suspended solid, and liquid (Fig. 1B). Each fraction was transferred to a different container

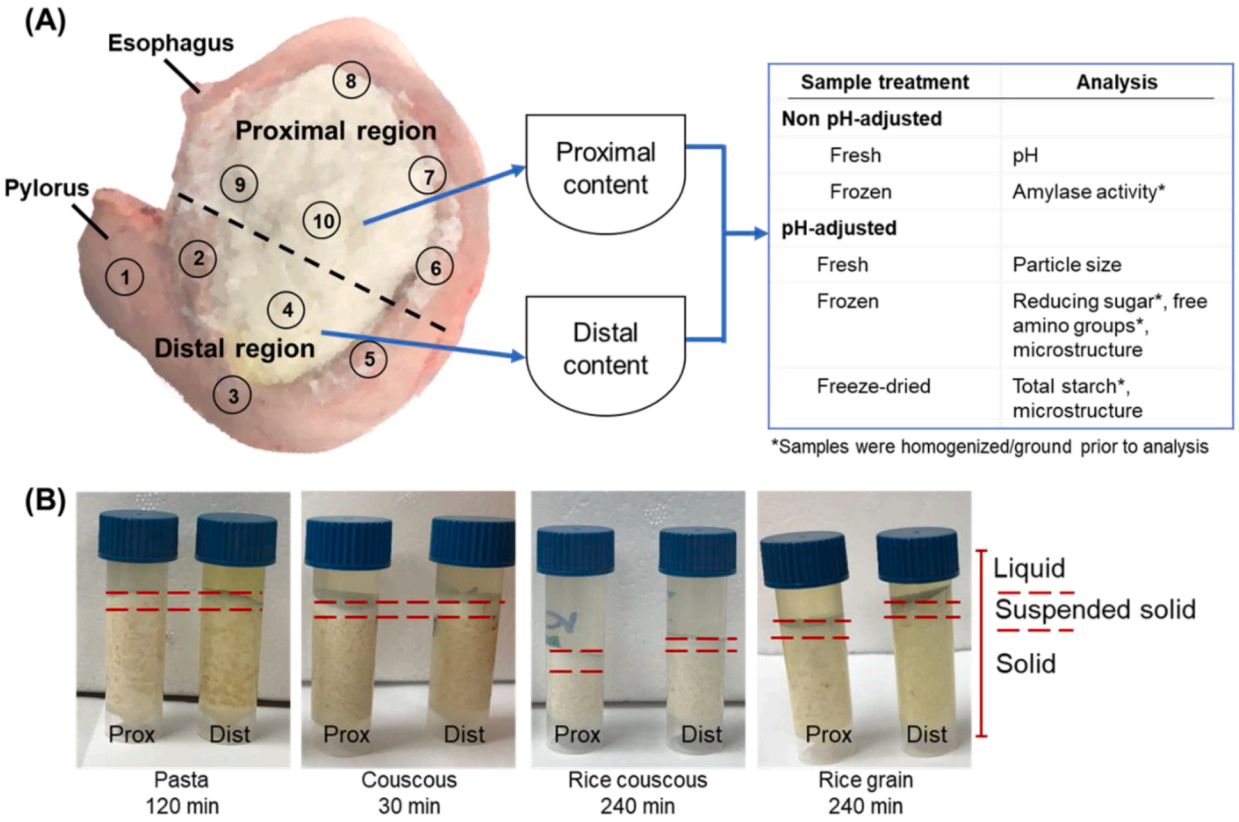

Fig. 1. (A) Example stomach with digesta and approximate pH measurement locations, with description of analyses done for each gastric sample. The dashed line indicates the approximate separation between proximal and distal stomach regions. (B) Examples of three fractions obtained after centrifugation of gastric digesta from the proximal (prox) or distal (dist) region when maximum separation was obtained. The approximate separation between fractions is indicated by dashed red lines. (For interpretation of the references to colour in this figure legend, the reader is referred to the web version of this article.)

and weighed. When the digesta fractions could be effectively separated, each digesta fraction was analyzed separately. Liquid and suspended solids were directly sampled for reducing sugar or free amino groups analysis. The solid fraction (containing particles larger than 5 mm) was homogenized using a handheld homogenizer (Scilogex D160 Homogenizer, Scilogex, Rocky Hill, CT, USA) at 8,000 rpm for 0.5–1 min to reach a slurry-like consistency, then sample from the homogenized solid was used for analysis. When solids, suspended solids, and liquids did not effectively separate after centrifugation (in 16 out of 90 rice noodle or rice grain digesta samples), the entire sample was treated as the solid fraction. For comparison to initial (undigested) condition, three batches of freeze-dried cooked diets were analyzed for reducing sugar and free amino groups. The undigested diets were treated as the solid fraction. Due to the large number of samples (282 digesta samples, most of them with 3 digesta fractions), reducing sugar and free amino group measurements were conducted on a single replicate for most samples. For each digesta fraction, one sample from every 12 samples was randomly selected for duplicate measurement to ensure the repeatability of the assay.

2.4.1.1. Reducing sugar assay. Reducing sugar content in the pH-adjusted digesta was quantified using the dinitrosalicylic acid (DNS) method (Miller, 1959), with modifications. The liquid fraction of the digesta was used directly for analysis. Reducing sugars from solid and suspended solid fractions were recovered by mixing 0.1 g solid (homogenized) or suspended solid sample with 1.5 mL water (equivalent to 1:15 solid/liquid ratio, w/v) on a vortex for 15 s. The mixtures were left undisturbed for 1 h at room temperature, then centrifuged (6,800 × *g*, 10 min) to separate the supernatant, which was used for analysis.

DNS reagent (0.4 mL) was mixed with 0.4 mL sample (maltose standard solution, liquid fraction, or supernatant from solid/suspended solid fractions), incubated in boiling water for 20 min, then cooled on ice for 10 min. Aliquots of sample (225 μL) were transferred to three wells of a 96-well microplate, and the absorbance was read on a microplate reader (SPECTROstar Nano, BMG Labtech, Ortenberg, Germany) at 540 nm. Reducing sugar content in the digesta was expressed as maltose equivalent, based on a maltose standard curve (0–2 mg maltose/mL), per gram digesta (referred to as mg maltose/g).

2.4.1.2. Free amino group content assay. Free amino groups in digesta fractions were quantified using the o-phtalaldehyde (OPA) method (Church, Porter, Catignani, & Swaisgood, 1985). The liquid fraction of the digesta was used directly for analysis. The solid and suspended solid fractions were prepared in the same way as the reducing sugar analysis, except that the addition of water was replaced with sodium tetraborate buffer (0.0125 M, with 2% SDS, pH 9). After 1 h of contact time with the buffer and centrifugation (6,800 × *g*, 10 min), the supernatant of the solid and suspended solid fractions were used for analysis. Aliquots of each sample (20 μL, liquid or supernatant from solid or suspended solid fraction) or glycine standard solutions were added to three wells of a 96-well microplate. OPA reagent or reagent blank (200 μL) was added and allowed to react for 3–4 min under minimum lighting. The absorbance was read on a microplate reader at 340 nm. Free amino group content in the samples was expressed as NH_2 equivalent, calculated from a glycine standard curve (0–0.5 mg glycine/mL sodium tetraborate buffer), per gram digesta (referred to as μg NH_2/g).

2.4.2. Apparent amylase activity assay

Apparent amylase activity in the gastric digesta was measured by modifying the original method for purified amylase (Bernfeld, 1955), where the non pH-adjusted digesta was treated as the starch substrate. Measurements were initially performed on digesta from all time points

for pasta, rice grain, rice noodle, and semolina. Results from these measurements indicated minimal activity at pH <2, therefore measurements on the remaining two diets were only performed on samples that had pH >2 (30-, 60-, and 120-min digesta for couscous; 30- and 60-min digesta for rice couscous).

Non pH-adjusted, frozen digesta samples were thawed in a water bath at 37 °C for 3 min, then the tubes were immediately placed in an ice bath. Samples were kept on ice at all times during the assay, unless otherwise stated, to minimize enzymatic activity that may occur after thawing frozen samples. Thawed samples (2–2.5 g) were transferred to another container, followed by addition of 20 mM sodium phosphate buffer containing 6.7 mM NaCl (1:2 w/v, digesta:buffer ratio). The pH of the buffer solution was adjusted to a pH similar to that of the specific digesta sample to be analyzed. In the ice bath, the mixture was homogenized at 8,000 rpm (Scilogex D160 Homogenizer, Scilogex, Rocky Hill, CT, USA) for 0.5–1 min to form a slurry. The resulting slurry was aliquoted (0.25 mL) to five microtubes, then diluted with 0.25 mL of the same buffer solution used for homogenization. The dilution was done to lower the starch concentration in the sample to enable the observation of amylase activity.

Diluted sample aliquots were immediately incubated for 0, 1, 2, 3, or 5 min in a water bath after 2 min equilibration at 37 °C. One aliquot was immediately removed after equilibration to represent the initial maltose concentration ($t = 0$ min). After incubation, each sample was immediately placed on ice for 10 min, then centrifuged at 6,800 × *g* for 10 min. The supernatant (0.1 mL) was diluted to 0.4 mL with water and mixed with 0.4 mL DNS reagent. Maltose content in the sample was determined as described in Section 2.4.1.1. When present, apparent salivary amylase activity in the sample was calculated from the slope of the linear portion of maltose vs. incubation time curve for each sample (example curves are given in Fig. S1). The apparent activity was expressed as the amount of maltose released per minute per gram digesta dry matter ((mg maltose//min)/g DM digesta) during 3 min incubation, as data points from 0 to 3 min exhibited a linear trend for most samples, in agreement with the original method (Bernfeld, 1955). Due to the large number of samples (total 215 samples × 5 incubation durations), duplicate measurements were conducted every 4 samples, and all other samples were analyzed with a single replicate.

2.4.3. Total starch content

Starch content of freeze-dried digesta samples (ground and sieved with a 1-mm sieve prior to analysis) was measured using the Megazyme Total Starch Kit (Megazyme, Wicklow, Ireland), following the procedure for samples not containing free glucose or maltodextrins. Analysis was conducted in batches of 10 unique samples, with two samples from each batch that were randomly selected for duplicate analysis to ensure the repeatability of the method, and the rest (8 samples) were analyzed with a single technical replicate due to the large number of samples. Gastric emptying of starch (i.e., starch content in digesta × dry matter of digesta from Nadia, Olenskyj, et al. (2021)) was determined using a modified power-exponential model for gastric emptying (Siegel et al., 1988):

$$\frac{X_t}{X_0} = 1 - \left(1 - e^{-k^* t}\right)^{\beta} \quad (1)$$

where X_t/X_0: starch remaining in the stomach at digestion time t (min) relative to the initial starch in the diet consumed (g DM starch in digesta/g DM starch in diet), k: the gastric emptying rate of starch in the dry matter of digesta (min^{-1}), and β: the theoretical y-intercept (unitless).

2.5. Particle size analysis

Particle size distribution (PSD) of the suspended solid fraction in pH-adjusted fresh digesta was determined using the Mastersizer-2000 (Malvern Instruments Ltd., Worcestershire, UK) following Bornhorst, Ferrua, Rutherfurd, Heldman, and Singh (2013), with a refractive index of 1.530 for starch-based samples (Angelidis, Protonotariou, Mandala, & Rosell, 2016). Couscous, semolina and rice couscous digesta were tested directly due to their liquid-like consistency. Pasta, rice grain, and rice noodle digesta contained many large particles, hence ~500 mg of sample was added to ~3 mL distilled water to allow small particles disperse, then the particle dispersion was analyzed. Digesta samples were analyzed in triplicate. Averaged PSD data from each diet × time × stomach region was fit to a lognormal function on DistFit software (DistFit™, Chimera Technologies Inc., Forest Lake, MN, USA) to analyze the multimodality of the distribution.

2.6. Microscopy analysis

2.6.1. Confocal microscopy

Microstructure of the diet and digesta were observed using a confocal laser scanning microscope (CLSM; Leica SP5 DM600B, Heidelberg, Germany). For each diet, frozen, cooked diets and representative samples of 60- and 240-min proximal and distal stomach digesta (from two pigs) were used for microscopy observation. The samples were thawed at 37 °C. Semolina and couscous samples were sampled directly, noodle samples were cut to 2.5 mm × 2.5 mm slices, and rice grain samples were cross-sectioned to 1 mm × 2 mm slices with a scalpel blade (Fig. S2). Protein and starch in the samples were double-stained using a mixture of FITC (20 μL, 1%-w/v in ethanol) and Rhodamine B (20 μL, 0.1% in ethanol) solutions, where FITC binds with both starch and protein due to the low protein concentration in the sample, while rhodamine B binds only with protein (Zheng, Stanley, Gidley, & Dhital, 2016). Samples were stained at least 90 min prior to observation. Prior to transferring to microscope slides, samples were washed 4 times with 1 mL distilled water to remove excess stains. During CLSM observation, a He-Ne laser was used with excitation wavelengths of 488 nm and 561 nm for FITC and rhodamine B, respectively.

2.6.2. Scanning electron microscopy (SEM)

Digesta samples (60 and 240 min, from two representative pigs for each diet) and cooked diets were freeze-dried, and a small portion of freeze-dried samples were affixed with double-faced adhesive tape on a metal stub. The samples were sputtered (SCD 050, Balzers, Liechtenstein) with gold for 200 s. Images were recorded with a scanning electron microscope (FEI ESEM Quanta 200, FEI Electron Optics, Eindhoven, The Netherlands) and observed at 20 kV accelerating voltage.

2.7. Statistical analysis

Statistical analysis was conducted using SAS®Studio 3.8 (SAS Institute, Cary, NC, USA). Only data points from pigs that consumed more than 50% of semolina or 70% of the other diets were used for analysis (Nadia, Olenskyj, et al., 2021). A multi-factor, mixed model ANOVA (PROC MIXED) was conducted on reducing sugar and amino group content, total starch, gastric pH, and PSD parameters. Each pig was an experimental unit, the diet type and digestion time were the between-subject factors, and the stomach region was the repeated factor within each pig. The batch of pigs was included as a main effect to account for interindividual variability. For pH data, the fraction of dry matter remaining in the stomach (from Nadia, Olenskyj, et al. (2021)) was included as an additional predictor due to better model fit (Akaike's information criteria) with the inclusion of this parameter (Bornhorst et al., 2014). Digesta fraction was used as an additional factor in the statistical model for reducing sugar and amino group content; it was nested within each stomach region (proximal or distal). When normality of residuals was not achieved for any dataset, the data was transformed. Preliminary statistical analysis with the mixed model was run to remove independent data points that were outside ± 3 internally studentized residuals, followed by the final statistical analysis on data sets with

outliers removed (Nadia, Olenskyj, et al., 2021). Differences between means where the main effects were significant were determined with Tukey-Kramer test at $p < 0.05$.

Averaged apparent amylase activity data at various pH ranges were analyzed using Kruskal-Wallis test; the differences between means at different pH ranges were determined with Dwass, Steel, Critchlow-Fligner test at $p < 0.05$. All values are reported as mean ± standard error of the mean (SE).

3. Results and discussion

3.1. Inhomogeneous intragastric pH distribution may extend remaining amylase activity during gastric digestion

Previous studies have suggested that gastric acidification kinetics may play an important role in meal digestion through modulation of gastrointestinal enzyme activity and dilution of the meal with gastric secretions, which could impact the overall rate of gastric breakdown and macronutrient hydrolysis (Bornhorst et al., 2014; Martens et al., 2020; Nau et al., 2022; Nau et al., 2019). To understand the links between these processes, the gastric acidification process of each diet was

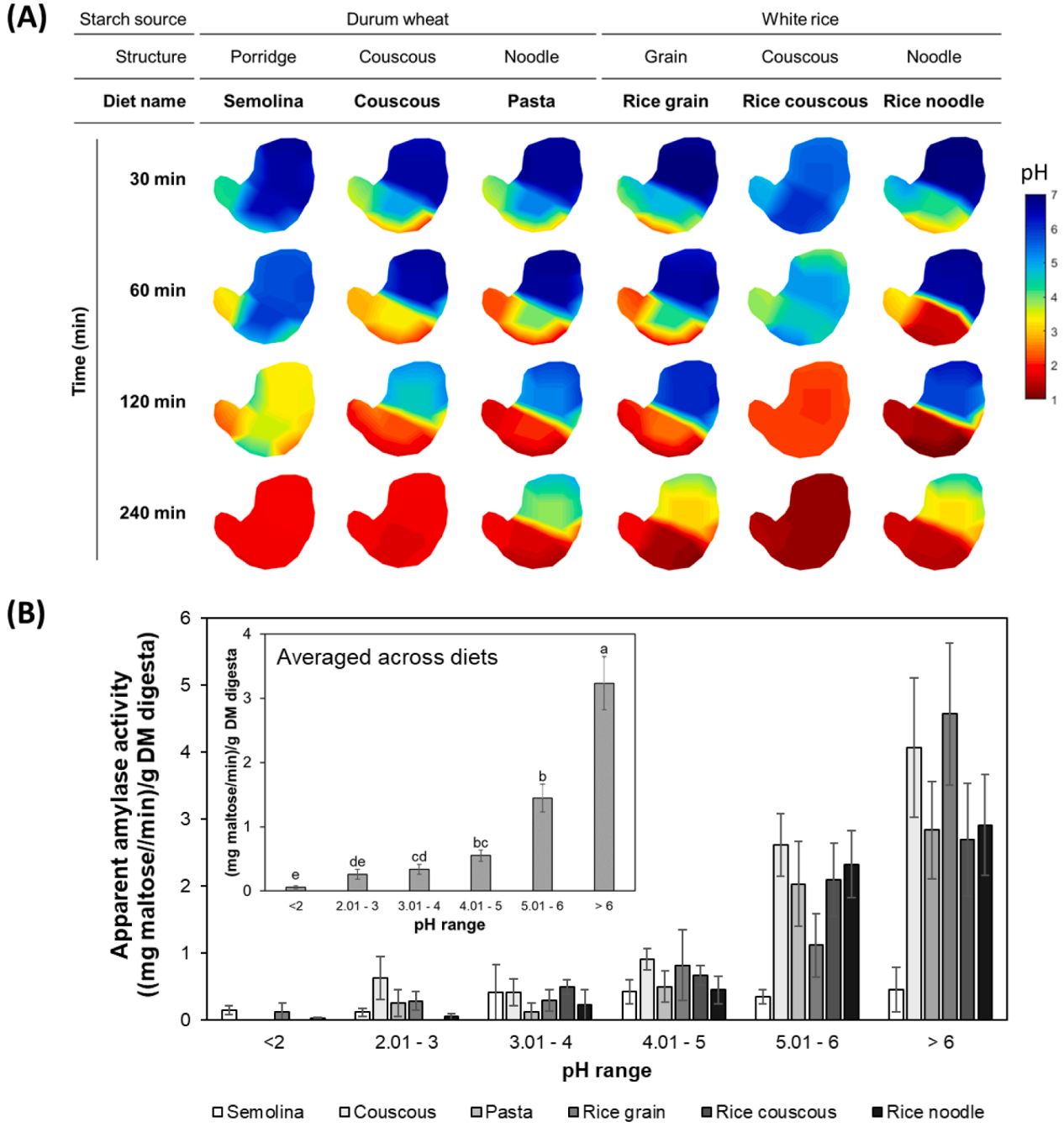

Fig. 2. (A) Color maps of intragastric pH distribution of the six experimental diets over 240 min gastric digestion (averaged from 4 to 6 pigs for each measurement location). Color maps for one diet type are located within the same column. The stomach shape was approximated from an image of a of full stomach from the study. (B) Apparent amylase activity at various digesta pH ranges for each diet. Averaged activity across diets is shown in the inset figure. Values in the inset figure. that share the same letters are not significantly different ($p < 0.05$). Values are presented as mean ± SE (n = 215 total data points).

estimated through visualization of the average intragastric pH from each of the 10 measurement locations (Fig. 2A; Table S3). The intragastric pH was significantly influenced by digestion time, measurement location, diet × measurement location, time × measurement location, diet × time × measurement location, and the batch of pigs ($p < 0.01$). Dry matter remaining was significant to the pH only when it interacted with measurement location, diet × measurement location, time × measurement location, and diet × time × measurement location ($p < 0.05$; Table S4). For all diets at all digestion times, a lower pH was observed near the pylorus (location 1), which might be attributed to higher contractile activity in the pylorus that enhanced mixing of the digesta with gastric secretions (Bornhorst, 2017). Locations 3 and 5 in the distal stomach also had a lower pH compared to the rest of the stomach, most likely due to the flow of gastric acid toward the pylorus and accumulation of gastric acid (produced in the proximal stomach) in these locations, similar to previous studies (Lærke & Hedemann, 2012; Nau et al., 2019). Based on the overall pH profile of the six diets by the end of 240 min (Fig. 2A), the diets could be classified into those that reached a uniform pH (semolina, couscous, and rice couscous) and those that had distinct pH separation within the stomach (pasta, rice grain, and rice noodle).

The group of diets that reached uniform pH were those with smaller initial particle size, compared to the diets that maintained a distinct pH gradient during the entire gastric digestion period (Fig. 2A, Table S2). It has been previously reported that during gastric digestion of the same six diets as the current study, there were similar differences in physical properties (e.g. rheological properties, texture) between the proximal and distal stomach across these two broad groups of diets. Those diets with larger particle size (pasta, rice grain, and rice noodle; Table S2) maintained larger differences in physical properties between the proximal and distal regions for longer gastric digestion times, which suggested lesser gastric mixing in these diets compared to those with smaller particle size (Nadia, Olenskyj, et al., 2021). These previously reported trends in gastric mixing and variations in gastric properties are supported by the results presented here, where larger intragastric pH gradients that were maintained during gastric digestion were present in the larger-sized diets. In contrast, the smaller-sized diets had more uniform physical properties and mixing with gastric secretions in the previously reported study as well as the current study. The combined results from these studies highlight the influence of food initial macrostructure and size on its acidification kinetics and mixing during gastric digestion (Nadia, Olenskyj, et al., 2021).

When the gastric acidification kinetics were examined in greater detail within the smaller-sized diets, semolina and rice couscous had less variations in their pH profiles compared to couscous. Couscous exhibited significantly higher pH in the proximal stomach compared to the distal stomach during the first 120 min of gastric digestion (5.17 ± 0.32 vs. 2.61 ± 0.24 in the proximal and distal stomach, respectively, averaged from 30 to 120 min, $p < 0.0001$), but reached a homogeneous intragastric pH at 240 min (1.95 ± 0.46 vs. 1.82 ± 0.42 in the proximal and distal stomach, respectively, $p = 1$). Among these three diets, the final pH of the digesta (averaged across measurement locations) was lower in rice couscous (1.29 ± 0.03), compared to couscous (1.84 ± 0.13) and semolina (1.85 ± 0.13). This difference was possibly due to the higher buffering capacity of couscous and semolina (55.26 and 74.48 μmol H^+/(g sample × ΔpH), respectively) compared to rice couscous (31.02 μmol H^+/(g sample × ΔpH)), as a result of higher protein content in the wheat-based diets. The effect of food buffering capacity on intragastric pH has been reported in previous gastric digestion studies using egg white gels (Nau et al., 2019), brown and white rice (Bornhorst et al., 2014), and liquid nutrient meals (Weinstein et al., 2013). In has been previously suggested that foods with higher buffering capacity elicit a greater gastric secretory response (Bornhorst, Chang, Rutherfurd, Moughan, & Singh, 2013; Nadia, Olenskyj, et al., 2021). However, foods with higher buffering capacity will also resist changes in pH with the addition of gastric secretions. As a result, the intragastric pH will vary based on the food buffering capacity, amount of gastric secretions, as well as the ease of mixing between the gastric secretions and the digesta.

When the gastric acidification kinetics were examined in detail for the larger-sized diets (pasta, rice grain, and rice noodle), there was an inhomogeneous pH profile, with a distinct intragastric pH gradient up to 240 min digestion. At 240 min, the pH of proximal stomach digesta (3.13 ± 0.26, averaged across the three diets) was still significantly higher ($p = 0.0022$) than the distal stomach digesta (1.58 ± 0.08). Variations between the larger-sized diets in their intragastric pH profiles even after 240 min of gastric digestion may reflect different extent of mixing and breakdown, in addition to different rates of gastric secretion addition to the diets during digestion due to their different buffering capacity values (Nadia, Olenskyj, et al., 2021). Similar pH gradients during digestion of egg white gels, rice, and almond have been previously observed in a pig model (Bornhorst et al., 2014; Nau et al., 2019).

It was hypothesized that the observed variations in gastric acidification kinetics between the six diets would affect the gastric amylase activity. Although amylase was not separated from the digesta, the relative apparent amylase activity was quantified in the gastric digesta (Fig. 2B, S3). The apparent activity ranged from 0 to 10.45 (mg maltose/min)/g DM digesta. This value is lower than salivary amylase activity reported in recent studies using specifically collected porcine or human saliva, with pre-gelatinized potato starch as the substrate (Freitas, Le Feunteun, et al., 2018; Martens et al., 2020). Porcine salivary amylase activity was found to have an optimal activity between pH 3 and 8.5, with a maximum activity equivalent to 154.0 (mg maltose/min)/mg DM saliva at pH 7.8 (Martens et al., 2020). Meanwhile, human salivary amylase activity was reported to have optimal activity between pH 3 and pH 7, with a maximum activity of 117.3 (mg maltose/min)/mL saliva at pH 6.2 (Freitas, Le Feunteun, et al., 2018).

The different procedure and units used to measure the enzyme activity (i.e., per saliva amount in previous studies vs. per digesta amount in this study), in addition to the difference in substrate (i.e., potato starch in previous studies vs. starch present in the digesta in this study) makes the specific values in this study difficult to compare with previous studies. However, the trend of decreasing amylase activity at lower pH in the present study was similar to those studies, suggesting that the method utilized in the current study may be useful to determine the relative amylase activity in gastric digesta. It should be noted that in the human stomach, gastric starch hydrolysis would primarily take place due to remaining activity of salivary amylase (Freitas, Le Feunteun, et al., 2018; Freitas, Souchon, et al., 2022). Meanwhile, in the pig, there may be contributions from both salivary amylases as well as bacterial amylases present in the pig stomach (Martens et al., 2020), such that the apparent amylase activity measured in the current study considers any amylase present in the digesta (not exclusively amylase from saliva).

Classification of the average apparent amylase activity across all diets based on pH range (Fig. 2B) showed that the apparent activity was the highest (3.23 ± 0.42 (mg maltose/min)/g DM digesta) at pH > 6. As the pH dropped to pH 5.01–6, the activity decreased to more than 50% of the highest activity (1.45 ± 0.22 (mg maltose/min)/g DM digesta), followed by gradual reduction as the pH became more acidic to an average of 0.06 ± 0.02 (mg maltose/min)/g DM digesta at pH <2. Although it is generally considered that salivary amylase becomes inactive at pH <3 (Brownlee et al., 2018), low amylase activity was still observed at pH between 2 and 4 in the present study. It is possible that oligosaccharides produced by amylolysis during early digestion times protected salivary amylase from inactivation by low pH and/or proteolysis by pepsin, likely due to specific binding of amylolysis products on the enzyme's active site (Rosenblum, Irwin, & Alpers, 1988). Variations between diets in the reduction of apparent amylase activity at lower pH might be attributed to different specificity of amylase on the starch sources, the enzyme affinity to the surface of the diets as affected by the diet and digesta structure (Dhital, Warren, Butterworth, Ellis, & Gidley, 2017), and different rate of gastric secretions and extent of mixing between the diets and gastric secretions (Nadia, Olenskyj, et al., 2021) that

may lead to different rates of enzyme inactivation.

Among the six diets, semolina exhibited the lowest apparent amylase activity even at pH >6 (0.45 ± 0.33 (mg maltose/min)/g DM digesta). This may be due to its porridge form and higher initial moisture content, which led to minimal mastication and lower saliva incorporation into the meal (Fig. 3A). Meanwhile, higher apparent amylase activity was found in the other diets at pH >6 (3.57 ± 0.43 (mg maltose/min)/g DM digesta, averaged across five diets at pH >6), which required longer time for mastication due to their larger initial particle size. This observation agrees with a mastication study that reported that food with softer texture and higher moisture content required less time for mastication, and that the amount of saliva added to food bolus decreased with increasing food initial moisture content (Motoi, Morgenstern, Hedderley, Wilson, & Balita, 2013). These findings also support the hypothesis that the apparent amylase activity measured in the current study mainly consisted of amylase from saliva due to variations in mastication of the diets, as opposed to bacterial amylases that may be found in the pig stomach (Martens et al., 2020).

3.2. *Consequences of intragastric pH profile on the chemical composition and microstructure of gastric digesta*

Based on the variations observed in intragastric pH distribution and apparent amylase activity between the diets (Fig. 2), it was hypothesized that those samples that had higher pH and greater apparent amylase activity would have greater starch hydrolysis during gastric digestion. Conversely, for those digesta samples with lower pH, it was hypothesized that there would be increased protein hydrolysis due to higher pepsin activity, which is active only at lower pH (Mennah-Govela, Swackhamer, & Bornhorst, 2021; Salelles, Floury, & Le Feunteun, 2021). To examine these hypotheses, the digesta was separated into three fractions (liquid, solid, and suspended solid) and each fraction was analyzed separately for maltose and NH_2 content as indicators of starch and protein hydrolysis, respectively (Fig. 4B-C). The different digesta fractions were analyzed separately because it was hypothesized that the suspended solid fraction in the digesta was mainly a result of starch hydrolysis by amylase that remained active in the stomach and digested the surface of the diets (Dhital et al., 2017); this caused leaching of smaller particles from the diet matrices, or erosion of the matrix surface which removed small particles, in agreement to what has been demonstrated in a static *in vitro* digestion study using similar diets to that of the current study (Nadia et al., 2022). Further, this hypothesis was supported by a higher maltose concentration in the suspended solid fraction compared to the liquid and solid fractions (i.e., 36.26 ± 1.55 mg/g suspended solid vs. 26.78 ± 1.06 mg/g liquid and 26.67 ± 1.20 mg/g solid, averaged across diet × digestion time × stomach region, $p < 0.0001$ for each comparison; Fig. 5), and the absence of differences in NH_2 content across the digesta fractions (Fig. 5).

The maltose concentration in the wet digesta was distributed across liquid, solid, and suspended solid fractions, and was significantly influenced by all factors and their interactions ($p < 0.05$), except any effects that included the stomach region × time interaction (Table S4).

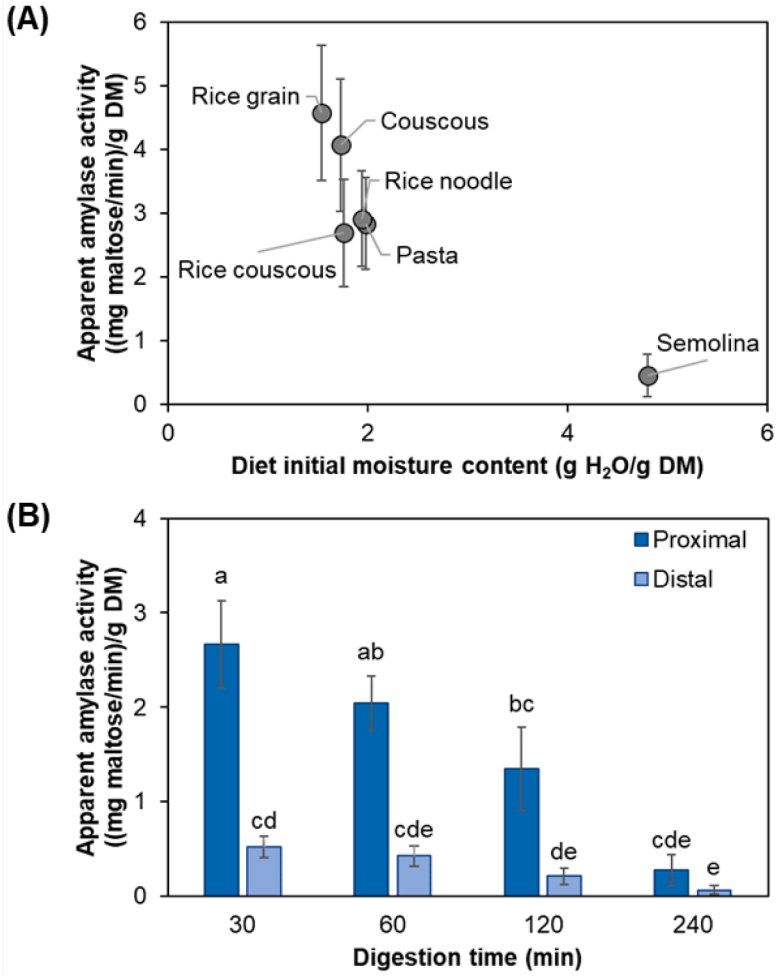

Fig. 3. Relationship between apparent amylase activity in gastric digesta with pH > 6 (n = 33 data points) and the initial moisture content of each diet (A). Apparent amylase activity at different digestion time points in the proximal and distal stomach, averaged across all diets (B). Values that shared the same letters are not significantly different ($p < 0.05$). All values are shown as means ± SE ($20 \leq n \leq 31$).

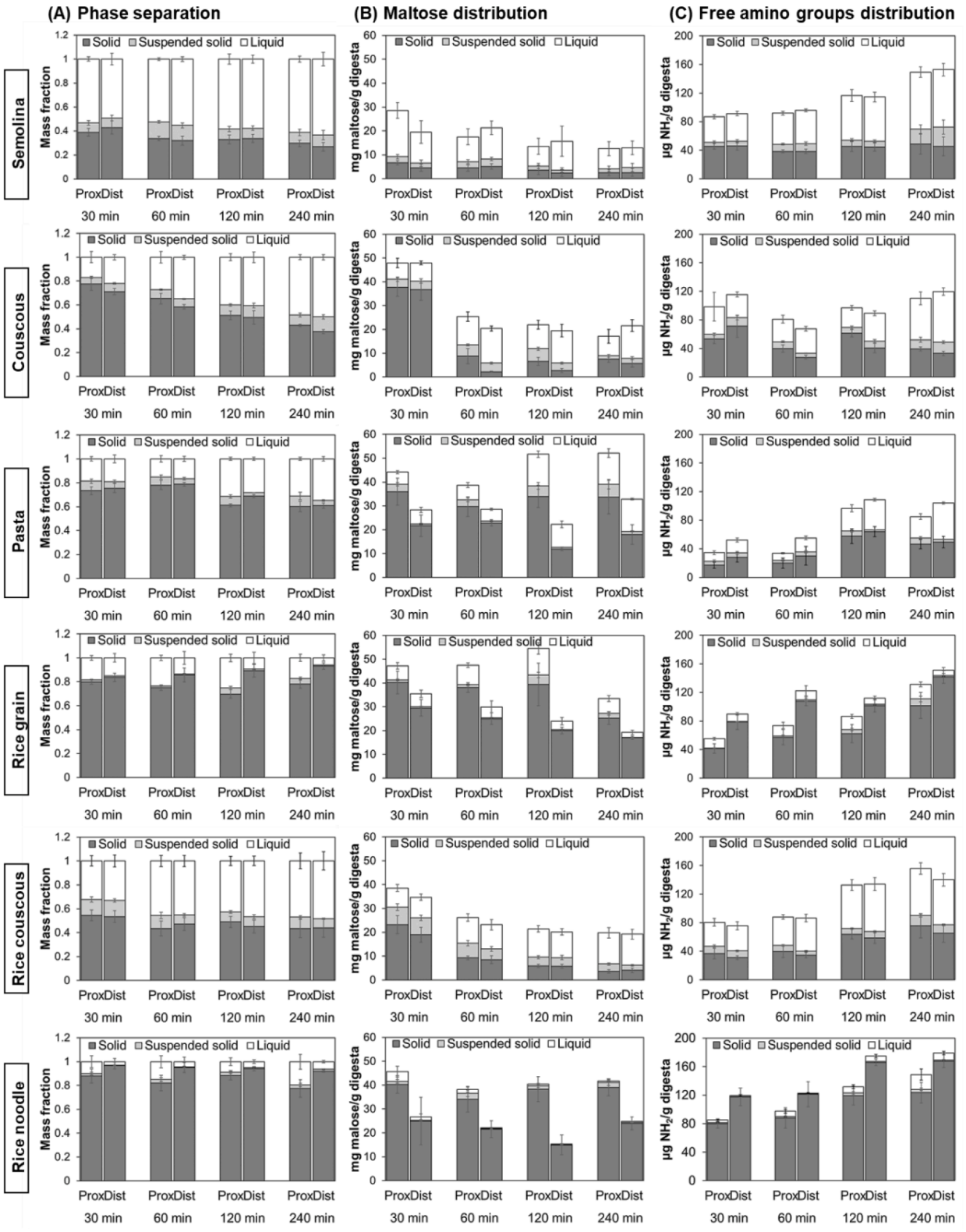

Fig. 4. Phase separation of digesta to different fractions (column A), and maltose (column B) and free amino groups (column C) distribution in wet digesta fractions during 240 min digestion in the proximal (Prox) and distal (Dist) stomach regions. Figures within the same row represent digesta for one diet. Bars for solid (dark grey), suspended solid (light grey), and liquid (white) fractions are shown within each digesta sample. Values are presented as mean ± SE ($5 \leq n \leq 6$ for each diet × time × stomach region × digesta fraction). Results are presented in digesta wet basis to enable the comparison across different digesta fractions.

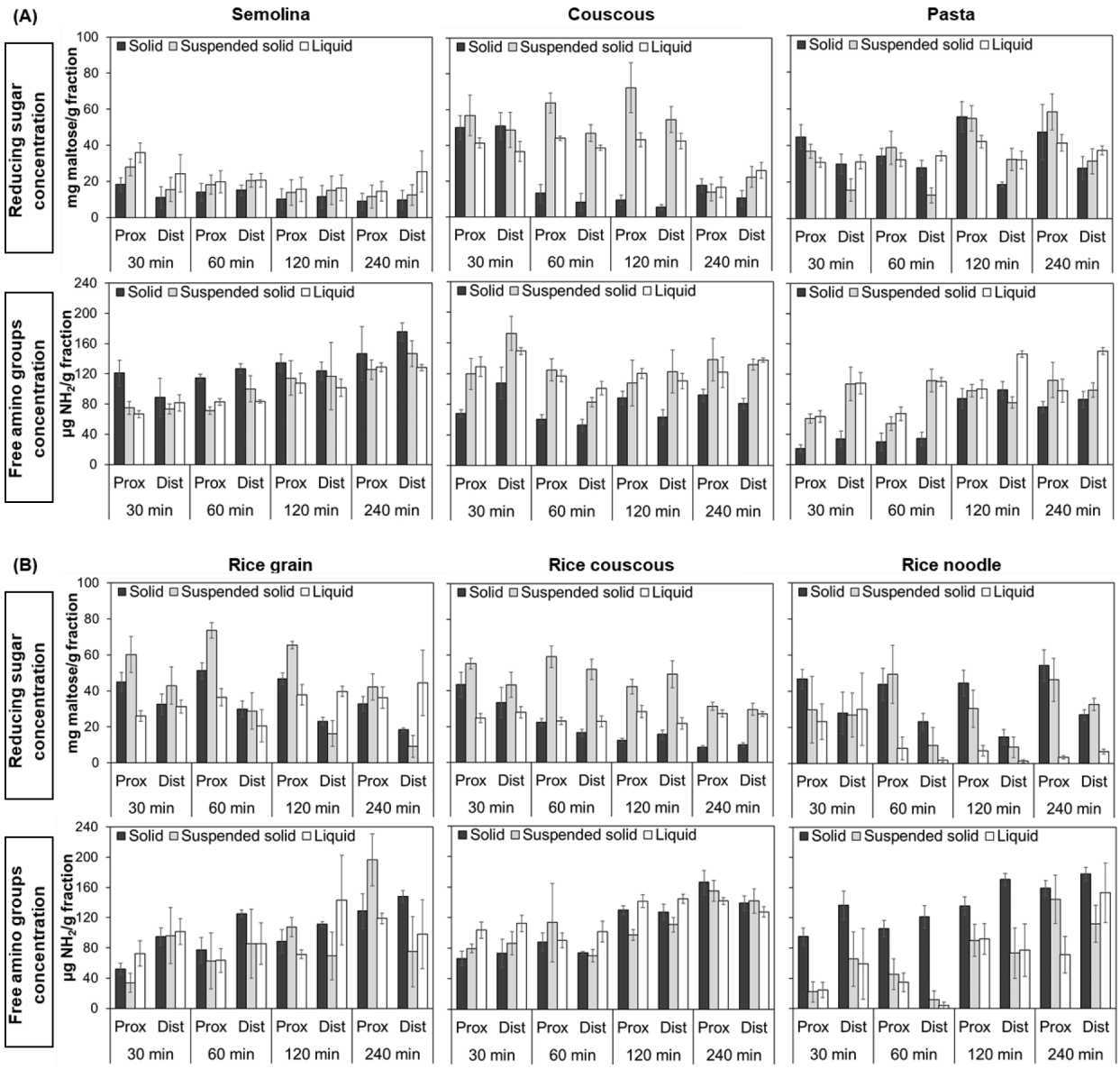

Fig. 5. Concentrations of maltose and free amino groups in different wheat-based (A) or rice-based (B) digesta fractions during 240 min digestion in the proximal (Prox) and distal (Dist) stomach regions. Figures within the same column of either wheat-based (A) or rice-based (B) diets represent the digesta composition for one diet type. Values are presented as mean ± SE ($5 \leq n \leq 6$ for each diet × time × stomach region × digesta fraction).

The total maltose concentration in the digesta (summed across digesta fractions) ranged from 12.60 to 54.56 mg/g (Fig. 4B), and was higher than the initial maltose concentration in the diets (1.68 ± 0.31 to 11.98 ± 0.93 mg/g; Table S2), indicating that starch hydrolysis occurred during gastric digestion. As an indirect indicator for starch hydrolysis, total maltose content was compared to the total starch content in digesta. The values ranged from 0.14 ± 0.01 to 0.32 ± 0.03 g maltose/g starch (calculated across proximal and distal stomach; Fig. 6), and were within the range of percent starch hydrolysis reported in previous *in vitro* digestion studies of various starch-rich foods (Freitas & Le Feunteun, 2019; Freitas et al., 2018; Nadia et al., 2022; Woolnough, Bird, Monro, & Brennan, 2010).

The starch hydrolysis observed in the gastric digesta samples was the combination of hydrolysis that occured during mastication and gastric digestion. The maximum value of starch hydrolysis was achieved after 30 min gastric digestion for all smaller-sized diets (i.e., not long after mastication), after 120 min for rice grain, and after 240 min for pasta and rice noodle. Since the starch hydrolysis increased during gastric digestion for larger-sized diets (Fig. 6), these diets likely underwent additional starch hydrolysis during gastric digestion. For the smaller-sized diets, the starch hydrolysis after 30 min gastric digestion may have occurred during either mastication or gastric digestion. However, the starch hydrolysis after mastication was not measured in the present study and represents a limitation in this analysis; this should be considered in future studies.

The starch hydrolysis during gastric digestion in larger-sized diets can be attributed to the higher pH in the proximal stomach, which led to higher apparent amylase activity in the proximal stomach up to 120 min digestion (averaged across digestion times and diets, $p < 0.05$, Fig. 3B). Consequently, the proximal stomach digesta of pasta, rice noodle, and rice grain had significantly higher ($p < 0.001$) total maltose concentration compared to the distal stomach (44.7 ± 1.7 vs. 25.6 ± 1.4 mg/g in the proximal and distal stomach, respectively, summed across digesta fractions and averaged across diet × time; Fig. 4B). In contrast, the total maltose concentration in the smaller-sized diets was not significantly different between stomach regions ($p = 0.8238$; Fig. 4B), as a result of their easier mixing with gastric secretions that led to more rapid inactivation of amylase. The greater mixing with gastric secretions can be

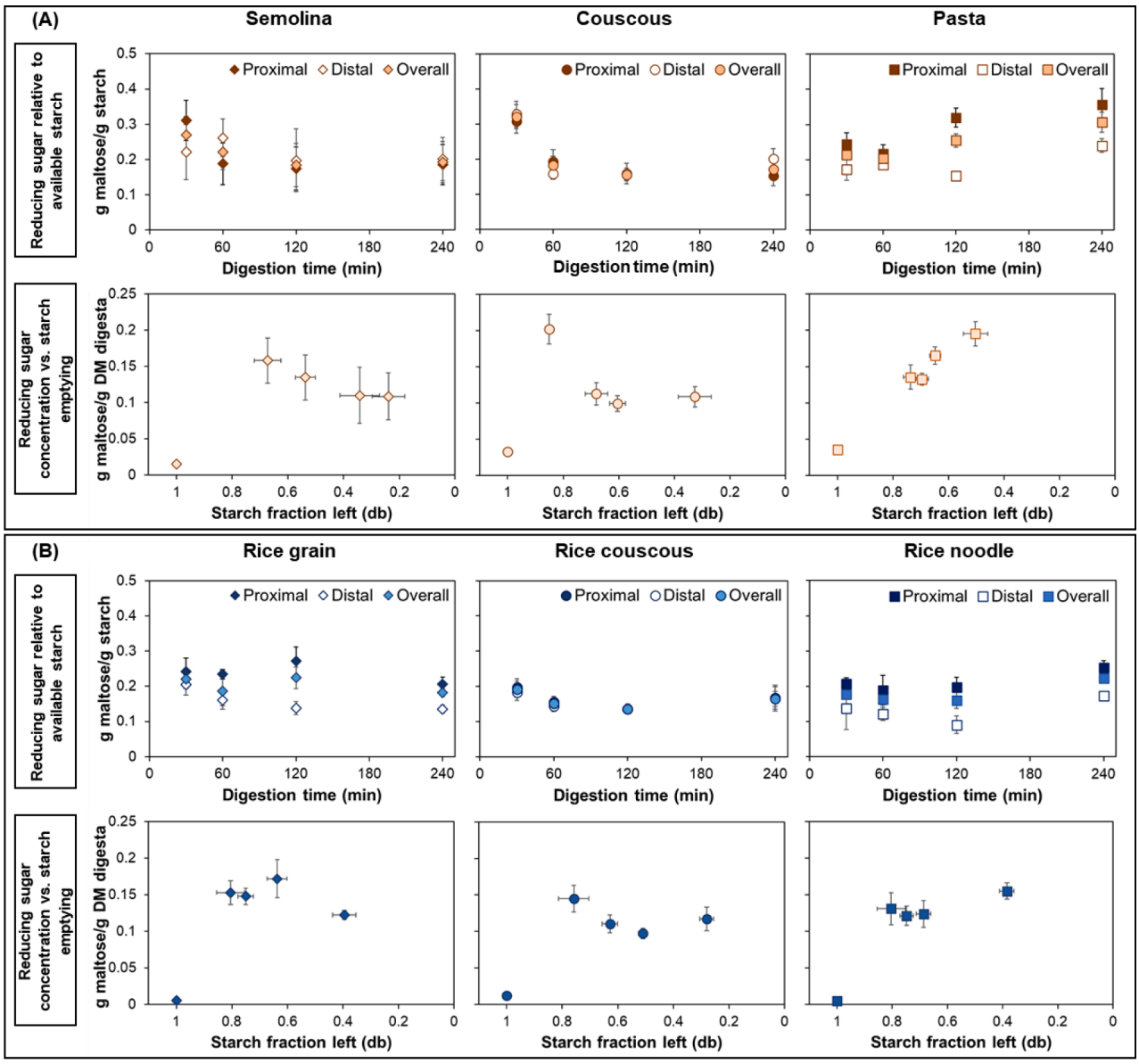

Fig. 6. Comparison between reducing sugar and starch in wheat-based (A) and rice-based (B) digesta expressed as total reducing sugar (summed across the digesta fractions) relative to total available starch in the proximal stomach, distal stomach, and overall stomach (proximal + distal combined) digesta (first row) or concentration of reducing sugar in digesta dry matter as a function of starch emptying profile (second row). The x-axis of starch fraction left is presented in a reversed order for easier tracking of the differences between hydrolyzed starch content in the digesta of larger- and smaller-sized diets as starch gastric emptying occurred. Figures within the same column represent data for one diet type. Values are presented as mean ± SE ($5 \leq n \leq 6$ for each data point shown in each graph).

seen as there was a higher proportion of the liquid fraction in the digesta of the smaller-sized diets (0.44 ± 0.02 vs. 0.18 ± 0.01, for smaller- vs. larger-sized diets, averaged across diet × stomach region × time; Fig. 4A).

The NH_2 concentration in the wet digesta was significantly influenced by all effects tested ($p < 0.05$), except diet × stomach region, stomach region × time × digesta fraction, and diet × stomach region × time × digesta fraction (Table S4). Although the percentage of protein hydrolysis was not calculated due to the low total protein content in the samples, gastric protein hydrolysis in the diets was suggested by higher NH_2 concentration in the solid and suspended solid fractions (ranging from 22.62 ± 4.82 to 169.20 ± 9.45 μg/g, summed across the two fractions; Fig. 4C) compared to the initial NH_2 concentration in the diets (0.12 ± 0.01 to 0.83 ± 0.11 μg/g, Table S2). The increasing NH_2 concentration in the liquid fraction over time might also indicate protein hydrolysis occurred during gastric digestion. However, there may be intereference from NH_2 in gastric secretions and saliva added during digestion to the NH_2 concentrations, which was not considered in this analysis, as it was not possible to collect separate samples of porcine saliva and gastric fluids as part of the current study.

The total NH_2 concentration was higher in the distal stomach digesta compared to the proximal stomach in pigs fed with pasta, rice grain, and rice noodle (89.6 ± 5.4 vs. 117.3 ± 5.4 μg/g in the proximal and distal stomach, respectively, averaged across diet × time × digesta fraction, $p < 0.001$). In contrast, the total NH_2 concentration in couscous, rice couscous, and semolina digesta were not significantly different between stomach regions (107.0 ± 4.1 vs. 107.0 ± 4.0 μg/g in the proximal and distal stomach, respectively, averaged across diet × time, $p = 0.9998$). The increase in NH_2 groups during digestion, and the increased NH_2 concentration in the distal region compared to the proximal region in the larger-sized diets was likely the result of protein hydrolysis by gastric pepsin. In contrast to amylase, which is active at pH >3, porcine gastric

pepsin has a maximum activity at pH 2, and is active at pH <4 (Mennah-Govela et al., 2021).

Consistent trends between smaller- and larger-sized diets in their maltose and NH_2 concentration between the proximal and distal stomach regions indicate the impact of variations in gastric mixing (Fig. 2A) on nutrient hydrolysis (starch and protein in this case), due to changes in intragastric pH and digestive enzyme activity. Variations in protein hydrolysis may be due to the influence of gastric mixing on pepsin activity. Although pepsin activity was not measured in the current study, previous studies have indicated that pepsin concentration may not be

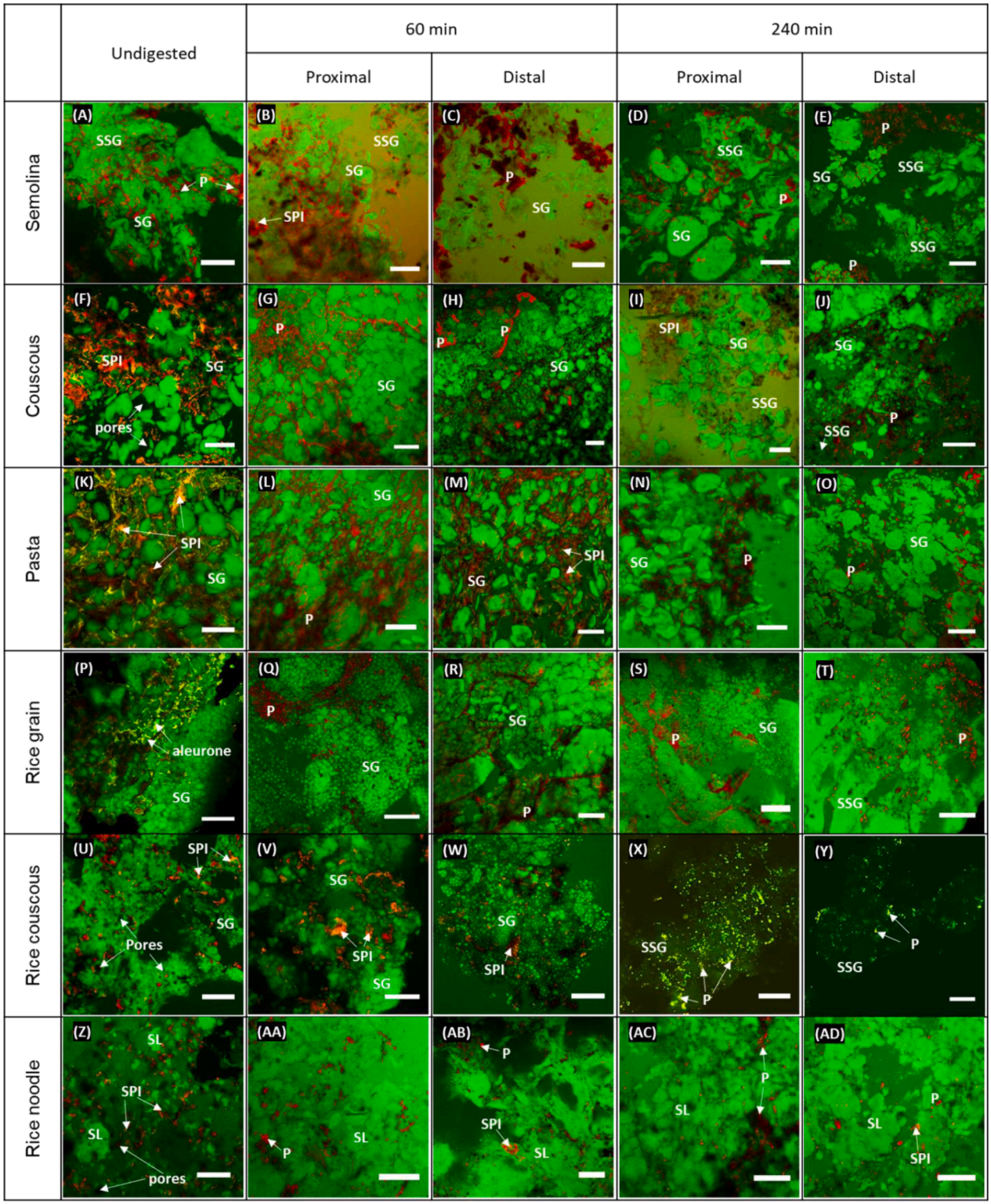

Fig. 7. Confocal scanning laser microscopy images of the six diets before digestion, and after 60- or 240-min digestion in the proximal and distal stomach regions from selected pigs. Starch component (in the form of starch granules (SG), starch lumps (SL), or solubilized starch granules (SSG)), protein (P), and starch-protein interaction (SPI), and are indicated by green, red, and yellow/orange color in the Fig., respectively. Scale bars represent 50 μm. (For interpretation of the references to colour in this figure legend, the reader is referred to the web version of this article.)

distributed in the same way as gastric secretions, and the protein hydrolysis is the result of a complex combination of gastric pH, pepsin concentration (Nau et al., 2022), and relative amount of food breakdown. As a result, pepsin concentration, pepsin activity, and their role in digesta protein hydrolysis should be investigated in future studies.

Although the main macronutrient in the diets used in the current study was starch, protein hydrolysis is particularly important for couscous, pasta, and rice grain that contained starch granules surrounded by a protein matrix (Fig. 7F, 7K, 7P). Hydrolysis of protein may affect the availability of starch granules for the subsequent small intestinal digestion and weaken the matrix structure, leading to increased breakdown (Freitas et al., 2018). Protein hydrolysis is less important to

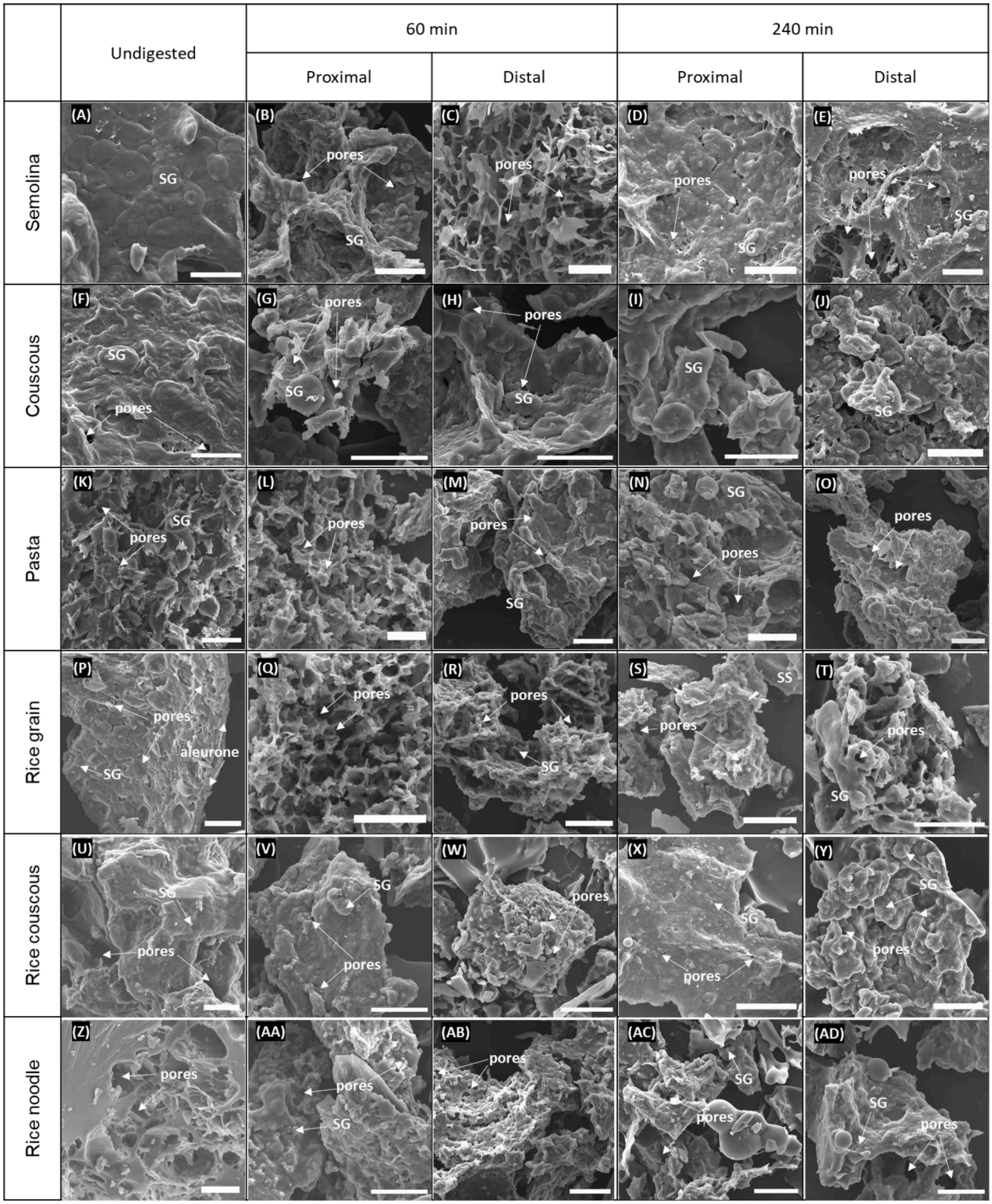

Fig. 8. Scanning electron microscope (SEM) images of the six diets before digestion, and after 60- or 240-min digestion in the proximal and distal stomach regions from selected pigs. Starch granules embedded in the matrix or leached into the surface of the diet or digesta are indicated with SG in the pictures, and examples of visible pores on the surface of the structures are shown. Scale bars represent 50 μm.

consider in the starch hydrolysis process of the other diets (semolina, rice couscous, rice noodle) that did not have encapsulation of starch granules in protein matrix, as the grinding processes to produce the fine particles in the raw materials disrupted the matrix, resulting in protein scattered between gelatinized starch network (Fig. 7).

To further understand how the starch and protein hydrolysis processes that occurred during gastric digestion were impacted by the diet initial structure and properties, microstructural changes in the diets and the digesta were observed (Fig. 7 and 8). Different arrangements of starch granules in the matrices of the diets were observed that may have impacted their susceptibility to enzymatic hydrolysis and breakdown during digestion: a mixture of solubilized and swollen starch with protein network interspersed between the matrix in semolina (Fig. 7A); swollen starch granules arranged between a protein-starch matrix and/or pores in couscous (Fig. 7F); swollen starch granules arranged tightly between starch-protein matrix in pasta (Fig. 7K); swollen starch granules in a constricted matrix, with scattered starch-protein interactions in rice grain (Fig. 7P); clusters of swollen starch granules within a porous matrix in rice couscous (Fig. 7U); and a gel matrix comprised of lumps of solubilized starch granules in rice noodle (Fig. 7Z) (Sangpring, Fukuoka, & Ratanasumawong, 2015; Tamura, Singh, Kaur, & Ogawa, 2016; Zou, Sissons, Gidley, Gilbert, & Warren, 2015). Each diet had different surface morphology (Fig. 8A, 8F, 8K, 8P, 8U, 8Z) and pores (except semolina). This may have facilitated diffusion of saliva and gastric secretions to increase enzymatic and acidic hydrolysis in the stomach (Wu et al., 2017).

During digestion, the starch-protein interactions that were initially present in wheat-based diets became less prevalent at longer digestion times (Fig. 7B-E, 7G-J, 7L-O), especially in the distal stomach, which might be due to hydrolysis of protein by pepsin, as evidenced by a general increase in NH_2 content in the digesta over time (Fig. 4C). For example, solubilization of starch granules was observed in couscous, rice couscous, and semolina at longer digestion times (Fig. 7D-E, 7I-J, 7X-Y) as a result of dilution of the digesta by gastric secretions over time (Fig. 4A and 9). Semolina was the only diet that had a limited number of pores in the undigested structure. However, pores were observed in semolina digesta (Fig. 8B-E), which might be due to digestion by amylase and acid hydrolysis. Changes on the surface of couscous and rice couscous digesta were also observed, with the presence of smaller fragments at longer digestion times (Fig. 8G-J, 8V-Y).

In pasta, rice grain, and rice noodle, the presence of more pores in the digesta (compared to the undigested structure; Fig. 8K-O, 8P-T, 8Z-AD) indicated that amylolysis (more pores and rough-surfaced layered structures) and acid hydrolysis (more pores and fragmented structures) occurred at least on the surface of the diets (Li et al., 2013). In some digesta samples, it was observed that starch granules or starch lumps were more swollen, possibly due to an increased uptake of digestive secretions into the digesta (Nadia, Olenskyj, et al., 2021). Nevertheless, these trends may not be fully representative of the whole digesta, as they were only observed on small samples that may have had varying pH and biochemical conditions, depending on their specific location in the stomach. Moreover, there might be artifacts due to sample preparation that can affect the interpretation of the observations. Microstructural changes during digestion in an *in vitro* system with controlled amounts of enzymes and digestive fluids merits future investigation to elucidate on the mechanisms and trends observed in the current study.

3.3. Modifications in the particle size distribution of the suspended solid digesta fraction

The PSD of large particles (>2 mm) of digesta from this study was presented in (Nadia, Olenskyj, et al., 2021) to investigate physical (macrostructural) breakdown during gastric digestion. In the current study, the PSD of suspended solid fraction of digesta (<2 mm) was investigated to reflect the impact of biochemical changes during digestion on the physical breakdown of diets that occurred as a surface phenomenon. The volume-mean diameter (D[4,3]), surface mean diameter (D[3,2]), and specific surface area (SSA) of the digesta were significantly influenced by diet type ($p < 0.0001$), stomach region and diet × stomach region interaction ($p < 0.05$), and batch of pigs ($p < 0.05$). Time was a significant variable for D[3,2] and SSA ($p < 0.05$). Diet × time was significant for D[4,3] and D[3,2] ($p < 0.05$). Limited trends can be observed in these PSD parameters (Table S5), although the SSA was expected to indicate differences, considering that starch hydrolysis is a surface phenomenon (Dhital et al., 2017). The 10th, 50th, and 90th percentile diameters (d_{10}, d_{50}, and d_{90}) were also quantified (Table S6). Nevertheless, these parameters may not sufficiently describe the changes in PSD during digestion due to the multimodality of the PSD (Fig. 10A-F). As such, additional particle size parameters were analyzed: location, spread, and volume of each peak (Table S7).

Visualization of the PSD of the suspended solid fraction showed that semolina, pasta, and rice noodle had three peaks, whereas couscous, rice couscous, and rice grain had up to four peaks in their distribution (Fig. 10A-F, Fig. S4). For wheat-based diets, the first peak occurred at between 4.6 and 9.4 μm; the second peak occurred at between 26.2 and 35.6 μm. The second peak location is close to the diameter of Durum wheat granules (20–25 μm) (Abecassis, Cuq, Boggini, & Namoune, 2012), thus particles occurring within the first peak range might be digested or dissolved starch granules. For rice-based diets, the first peak occurred at between 4.4 and 14.6 μm, which is within the range of rice starch granule diameter (3–15 μm) (Ramadoss et al., 2019); the second peak appeared at between 11.3 and 152.8 μm. Across all six diets, the third peak occurred between 85.3 and 959.6 μm; and the fourth peak (when present) occurred between 425.5 and 918.6 μm. It was hypothesized that the occurrence of peaks not attributed to starch granules might be attributed to surface erosion (due to starch hydrolysis), and chipping and fragmentation of digesta particles (Drechsler & Ferrua, 2016) due to mechanical breakdown (either by gastric contractions or friction between particles in the stomach). Different PSD profiles between the diets and their changes over time were hypothesized to be correlated with the extent of biochemical breakdown in the stomach, gastric emptying, and subsequent intestinal digestion. However, simultaneous mechanical breakdown, gastric secretion addition, and material emptying that occurred in addition to biochemical breakdown (Nadia, Olenskyj, et al., 2021), as well as dissolution of the particles into the dispersing agent during measurement, may have interfered with the PSD results from the suspended solid fraction, thus limiting the interpretation of the observations.

3.4. Link between starch hydrolysis during gastric digestion with physical breakdown of the diets and gastric emptying of starch

The process of gastric digestion involves the physical breakdown of food macrostructure, mixing and dilution with gastric secretions, enzymatic and acidic hydrolysis of food components, and ultimately gastric emptying of the digesta. As the current study focused on the importance of these processes in gastric starch digestion, the gastric emptying of starch was also compared to link to the trends observed in gastric pH, amylase activity, starch hydrolysis, and the particle size of the suspended solid fraction. The gastric emptying of starch was significantly influenced by diet type, time, and diet × time interaction ($p < 0.01$). Starch emptying half-time ($t_{1/2,starch\ GE}$) of the diets ranged from 71 min (semolina) to 275 min (pasta), where smaller-sized diets had shorter $t_{1/2,starch\ GE}$ (71 to 146 min) than the larger-sized diets (180 to 275 min). The $t_{1/2,starch\ GE}$ had the same order to a previously reported trend in dry matter gastric emptying half-time for the same diets (Nadia, Olenskyj, et al., 2021). Distinction in the $t_{1/2,starch\ GE}$ between smaller- and larger-sized diets signifies the impact of food initial macrostructure not only on gastric mixing, but also starch emptying rate, by affecting the physical breakdown mechanisms.

Semolina, couscous and rice couscous had small initial particle size (d <2 mm); they did not require extensive mechanical breakdown prior

to gastric emptying and were able to be emptied more easily. It was hypothesized that the gastric emptying of the smaller-sized diets was primarily controlled by meal dilution or dissolution by gastric secretions. This can be seen by the consistently increasing liquid proportion in phase separation of their digesta (Fig. 9) as a result of solid emptying and more addition of gastric secretions. In contrast, pasta, rice grain, and rice noodle had larger initial particle size, and they were reported to have physical breakdown rates (quantified as softening half-times) that were at least a magnitude higher than those of smaller-sized diets (Nadia, Olenskyj, et al., 2021). Consequently, their starch emptying process may have been limited by the rate of physical breakdown rather than the rate of dilution or dissolution by gastric secretions. In the digesta of larger-sized diets, there was more solid fraction (a mixture of dry matter, moisture in the cooked diet, and absorbed gastric secretions) compared to the liquid and suspended solid fractions at all digestion times (Fig. 9). Biochemical breakdown during gastric digestion was hypothesized to aid their physical breakdown by weakening the food matrix (through diffusion of gastric secretions and enzymatic processes) and eroding the surface of the diets (through enzymatic processes) to generate the suspended solid fraction. The suspended solid fraction, together with liquid fraction, might contribute to ensuring constant material emptying from the stomach (as observed in their starch emptying profile; Fig. 10G) – since gastric emptying process prioritizes liquid and particles <2 mm, or occasionally up to 7 mm (Coupe, Davis, Evans, & Wilding, 1991).

Interestingly, while starch was emptied over time for all diets, the concentration of maltose in digesta (which was expected to decrease as a result of secretion addition and gastric emptying) did not decrease until 120 min digestion for rice grain, or did not decrease at any digestion time for pasta and rice noodle (Fig. 6). This suggests an accumulation of starch hydrolysis products in the stomach for larger-sized diets, which

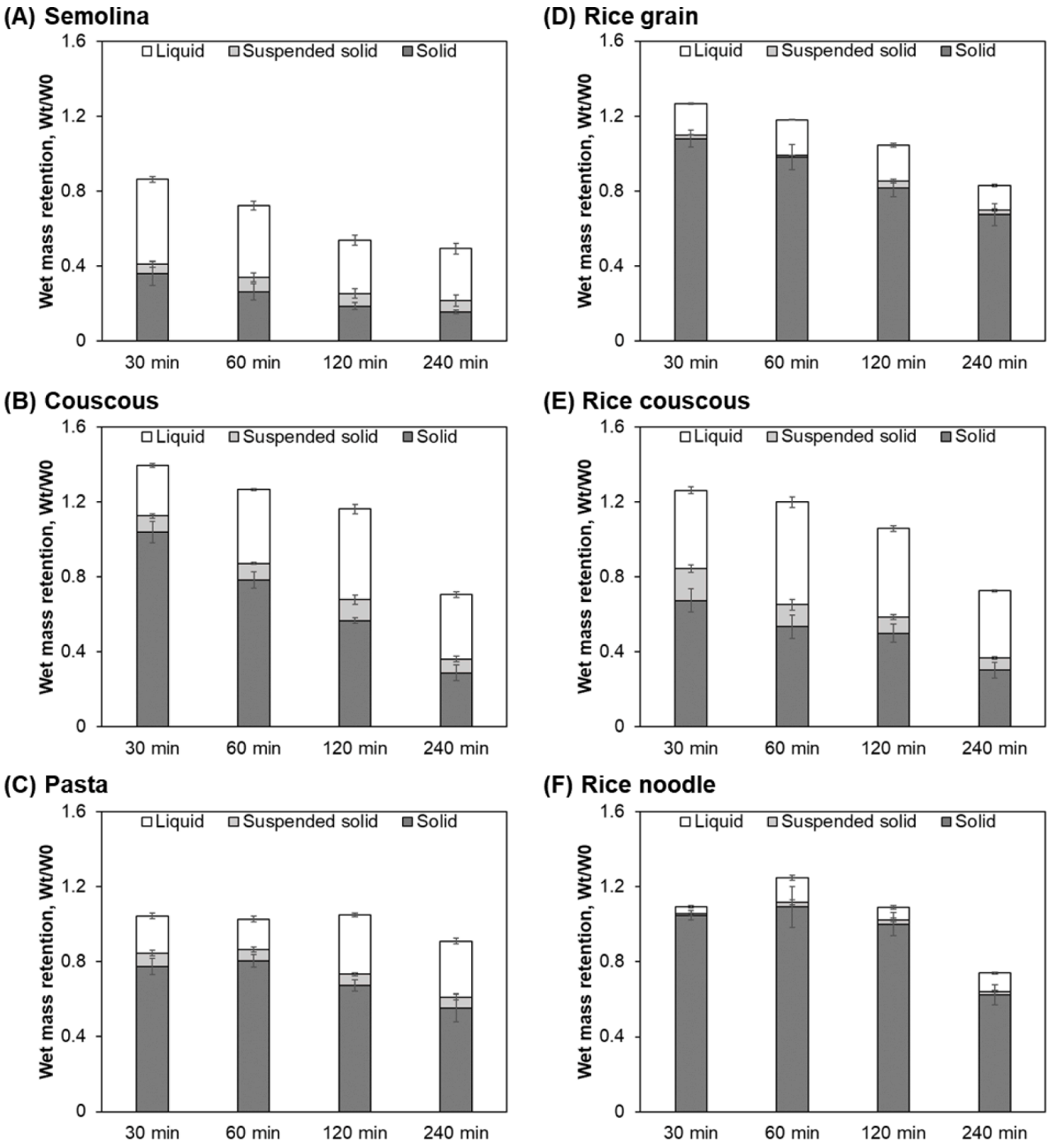

Fig. 9. Wet mass retention of digesta integrated with the phase separation data (Fig. 4A) to estimate the total fraction (on a wet basis) of liquid, suspended solids, and solids in digesta of (A) semolina, (B) couscous, (C) pasta, (D) rice grain, (E) rice couscous, and (F) rice noodle. Wet mass retention data was obtained from Nadia, Olenskyj, et al. (2021). Values are shown as mean ± SE ($4 \leq n \leq 6$ for each individual component of each bar graph).

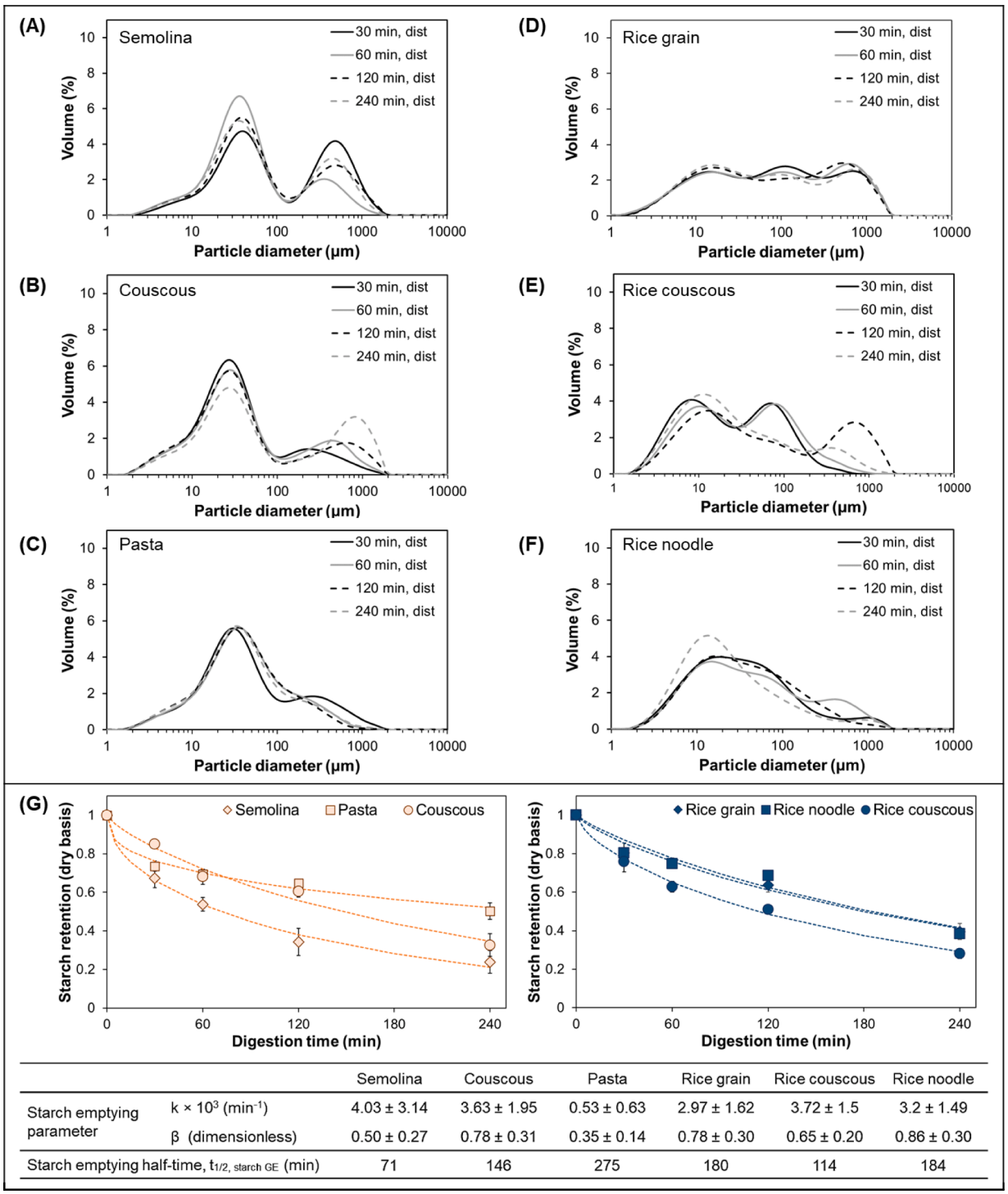

		Semolina	Couscous	Pasta	Rice grain	Rice couscous	Rice noodle
Starch emptying parameter	$k \times 10^3$ (min^{-1})	4.03 ± 3.14	3.63 ± 1.95	0.53 ± 0.63	2.97 ± 1.62	3.72 ± 1.5	3.2 ± 1.49
	β (dimensionless)	0.50 ± 0.27	0.78 ± 0.31	0.35 ± 0.14	0.78 ± 0.30	0.65 ± 0.20	0.86 ± 0.30
Starch emptying half-time, $t_{1/2,\ starch\ GE}$ (min)		71	146	275	180	114	184

Fig. 10. Particle size distribution of the suspended solid fraction of distal (dist) gastric digesta of pigs fed with (A) semolina, (B) couscous, (C) pasta, (D) rice grain, (E) rice couscous, and (F) rice noodle from 30 to 240 min gastric digestion. Curves represent the average from 4 to 6 pigs. (G) Starch gastric emptying profiles of wheat-based (left) and rice-based (right) diets during 240 min gastric digestion. Each data point represents mean ± SE ($5 \leq n \leq 6$). Dashed lines indicate the predicted starch emptying profile based on obtained gastric emptying parameters (listed in the table below the graphs; predicted parameter ± 95% confidence interval) from fitting of data from each diet to Eq. (1). Starch emptying half-time was calculated by fitting the gastric emptying parameters to Eq. (1) to obtain $X_t/X_0 = 0.5$.

can be attributed to extended amylase activity in the proximal stomach due to slower gastric mixing. The accumulation might also be enhanced by slower delivery of materials (a mixture of mostly starch and hydrolysis products, together with other non-starch components) to the small intestine, which might also impact physiological responses related to gastric emptying that were not measured in this study. For example, a negative feedback mechanism by the presence of hydrolyzed starch or glucose in the small intestine was reported to reduce gastric emptying rate (Brener, Hendrix, & McHugh, 1983; Lin, Kim, Elashoff, Doty, Gu, & Meyer, 1992).

Finally, the different $t_{1/2,starch\ GE}$ of the six diets, and the maltose content of the emptied fractions were expected to affect the subsequent

intestinal digestion and glucose absorption, which were outside the scope of this study. The liquid and suspended solid fractions of digesta from smaller-sized diets contained higher maltose concentration than those of larger-sized diets (14.58 ± 0.74 vs. 7.15 ± 0.64 mg/g digesta, respectively, averaged across diet × time for each diet classification, $p < 0.0001$; Table S8). Combined with the shorter $t_{1/2,\text{starch GE}}$ of smaller-sized diets, this might imply there was a high rate of delivery of starch and its hydrolysis products to the small intestine for couscous, rice couscous, and semolina, which might impact the rate of small intestinal digestion and glucose absorption. Findings from clinical and *in vitro* dynamic digestion studies on various couscous products showed that millet couscous had a slow gastric emptying rate and slower starch hydrolysis during gastric digestion compared to wheat couscous, resulting in lower glycemic response in humans (Cisse, Erickson, Hayes, Opekun, Nichols, & Hamaker, 2018; Hayes et al., 2020). Therefore, it was expected that diets with smaller particle size and easier mixing with gastric secretions would result not only in faster emptying of starch and its hydrolysis products, but also more rapid conversion to glucose in the small intestine, and subsequently higher glycemic response. The relationship between food structure, physical and biochemical changes during gastric digestion, and small intestinal digestion merits future investigation.

4. Conclusions

The present study demonstrated the effect of initial macrostructure of food on the biochemical environment for starch hydrolysis in the proximal and distal stomach regions, and its possible contribution to starch emptying mechanisms of foods. Diets with larger particle size (pasta, rice grain, and rice noodle) showed higher intragastric pH in the proximal stomach digesta compared to that of the distal stomach until 240 min gastric digestion. Consequently, the digesta from larger-sized diets had an extended period of salivary amylase activity in the proximal stomach, which resulted in increased starch hydrolysis that might aid their physical breakdown through biochemical digestion by producing particles <2 mm identified as the suspended solid fraction, to ensure starch could be emptied from the stomach. The gastric digesta from diets with smaller particle size (couscous, rice couscous, and semolina) had a uniform pH by the end of 240 min digestion. They had more rapid gastric content acidification by gastric secretions and faster inactivation of amylase. However, these diets had high starch hydrolysis after 30 min gastric digestion, which possibly occurred during mastication or extended amylolysis in the early stages of gastric digestion. The different maltose content in the liquid and suspended solid fraction of the digesta of the large and smaller-sized diets due to starch hydrolysis during gastric digestion might affect the subsequent small intestinal digestion and glucose absorption, which should be investigated in future studies.

CRediT authorship contribution statement

Joanna Nadia: Methodology, Formal analysis, Investigation, Writing – original draft, Writing – review & editing, Visualization. **Alexander G. Olenskyj:** Investigation, Writing – review & editing. **Parthasarathi Subramanian:** Methodology, Formal analysis, Writing – review & editing. **Suzanne Hodgkinson:** Methodology, Investigation, Writing – review & editing. **Natascha Stroebinger:** Methodology, Investigation, Writing – review & editing. **Talia G. Estevez:** Methodology, Formal analysis. **R. Paul Singh:** Writing – review & editing. **Harjinder Singh:** Funding acquisition, Writing – review & editing. **Gail M. Bornhorst:** Conceptualization, Methodology, Investigation, Writing – review & editing, Supervision, Project administration.

Declaration of Competing Interest

The authors declare that they have no known competing financial interests or personal relationships that could have appeared to influence the work reported in this paper.

Acknowledgments

This project was funded by the Tertiary Education Commission with grant number Center of Research Excellence – Riddet Institute (ref: A914656). The authors acknowledge the Riddet Institute Nutrition Team, Dr. Eric Neumann, and technical staff for their contribution in the animal handling and sampling during the animal treatment period. The authors also thank Dr. Carlos Montoya (Riddet Institute and AgResearch) and Dr. Jonathan Godfrey (Massey Statistical Consultancy Service) for their advice on the statistical analysis.

Appendix A. Supplementary data

Supplementary data to this article can be found online at https://doi.org/10.1016/j.foodchem.2022.133410.

References

Abecassis, J., Cuq, B., Boggini, G., & Namoune, H. (2012). Other traditional durum-derived products. In M. Sissons, J. Abecassis, B. Marchylo, & M. Carcea (Eds.), *Durum wheat: Chemistry and technology*. Minnesota, USA: AACC International.

Angelidis, G., Protonotariou, S., Mandala, I., & Rosell, C. M. (2016). Jet milling effect on wheat flour characteristics and starch hydrolysis. *Journal of Food Science and Technology, 53*(1), 784–791. https://doi.org/10.1007/s13197-015-1990-1

Bernfeld, P. (1955). Amylases, α and β. In *Methods in Enzymology* (pp. 149–158). Academic Press.

Bornhorst, G. M. (2017). Gastric mixing during food digestion: Mechanisms and applications. *Annual Review of Food Science and Technology, 8*, 523–542. https://doi.org/10.1146/annurev-food-030216-025802

Bornhorst, G. M., Chang, L. Q., Rutherfurd, S. M., Moughan, P. J., & Singh, R. P. (2013). Gastric emptying rate and chyme characteristics for cooked brown and white rice meals in vivo. *Journal of the Science of Food and Agriculture, 93*(12), 2900–2908. https://doi.org/10.1002/jsfa.6160

Bornhorst, G. M., Ferrua, M. J., Rutherfurd, S. M., Heldman, D. R., & Singh, R. P. (2013). Rheological properties and textural attributes of cooked brown and white rice during gastric digestion in vivo. *Food Biophysics, 8*(2), 137–150. https://doi.org/10.1007/s11483-013-9288-1

Bornhorst, G. M., Rutherfurd, S. M., Roman, M. J., Burri, B. J., Moughan, P. J., & Singh, R. P. (2014). Gastric pH distribution and mixing of soft and rigid food particles in the stomach using a dual-marker technique. *Food Biophysics, 9*(3), 292–300. https://doi.org/10.1007/s11483-014-9354-3

Brener, W., Hendrix, T. R., & McHugh, P. R. (1983). Regulation of the gastric emptying of glucose. *Gastroenterology, 85*(1), 76–82.

Brownlee, I. A., Gill, S., Wilcox, M. D., Pearson, J. P., & Chater, P. I. (2018). Starch digestion in the upper gastrointestinal tract of humans. *Starch-Stärke, 70*(9–10), 1700111. https://doi.org/10.1002/star.201700111

Church, F. C., Porter, D. H., Catignani, G. L., & Swaisgood, H. E. (1985). An o-phthalaldehyde spectrophotometric assay for proteinases. *Analytical Biochemistry, 146*(2), 343–348. https://doi.org/10.1016/0003-2697(85)90549-4

Cisse, F., Erickson, D. P., Hayes, A. M. R., Opekun, A. R., Nichols, B. L., & Hamaker, B. R. (2018). Traditional Malian solid foods made from sorghum and millet have markedly slower gastric emptying than rice, potato, or pasta. *Nutrients, 10*, 124. https://doi.org/10.3390/nu10020124

Coupe, A. J., Davis, S. S., Evans, D. F., & Wilding, I. R. (1991). Correlation of the gastric emptying of nondisintegrating tablets with gastrointestinal motility. *Pharmaceutical Research, 8*(10), 1281–1285. https://doi.org/10.1023/a:1015855829864

Dhital, S., Warren, F. J., Butterworth, P. J., Ellis, P. R., & Gidley, M. J. (2017). Mechanisms of starch digestion by α-amylase-Structural basis for kinetic properties. *Critical Reviews in Food Science and Nutrition, 57*(5), 875–892. https://doi.org/10.1080/10408398.2014.922043

Drechsler, K. C., & Ferrua, M. J. (2016). Modelling the breakdown mechanics of solid foods during gastric digestion. *Food Research International, 88*, 181–190. https://doi.org/10.1016/j.foodres.2016.02.019

Freitas, D., Boué, F., Benallaoua, M., Airinei, G., Benamouzig, R., & Le Feunteun, S. (2021). Lemon juice, but not tea, reduces the glycemic response to bread in healthy volunteers: A randomized crossover trial. *European Journal of Nutrition, 60*, 113–122. https://doi.org/10.1007/s00394-020-02228-x

Freitas, D., Boué, F., Benallaoua, M., Airinei, G., Benamouzig, R., Lutton, E., … Le Feunteun, S. (2022). Glycemic response, satiety, gastric secretions and emptying after bread consumption with water, tea or lemon juice: A randomized crossover intervention using MRI. *European Journal of Nutrition*. https://doi.org/10.1007/s00394-021-02762-2

Freitas, D., & Le Feunteun, S. (2018). Acid induced reduction of the glycaemic response to starch-rich foods: The salivary α-amylase inhibition hypothesis. *Food & Function, 9*(10), 5096–5102. https://doi.org/10.1039/C8FO01489B

Freitas, D., & Le Feunteun, S. (2019). Oro-gastro-intestinal digestion of starch in white bread, wheat-based and gluten-free pasta: Unveiling the contribution of human

salivary α-amylase. *Food Chemistry, 274*, 566–573. https://doi.org/10.1016/j.foodchem.2018.09.025

Freitas, D., Le Feunteun, S., Panouille, M., & Souchon, I. (2018). The important role of salivary alpha-amylase in the gastric digestion of wheat bread starch. *Food & Function, 9*(1), 200–208. https://doi.org/10.1039/c7fo01484h

Freitas, D., Souchon, I., & Le Feunteun, S. (2022). The contribution of gastric digestion of starch to the glycaemic index of breads with different composition or structure. *Food & Function, 13*(4), 1718–1724. https://doi.org/10.1039/D1FO03901F

Hayes, A. M. R., Swackhamer, C., Mennah-Govela, Y. A., Martinez, M. M., Diatta, A., Bornhorst, G. M., & Hamaker, B. R. (2020). Pearl millet (Pennisetum glaucum) couscous breaks down faster than wheat couscous in the Human Gastric Simulator, though has slower starch hydrolysis. *Food & Function, 11*(1), 111–122. https://doi.org/10.1039/C9FO01461F

Holmes, R. (1971). Carbohydrate digestion and absorption. *Journal of Clinical Pathology. Supplement (Royal College of Pathologists), 5*, 10–13. https://www.ncbi.nlm.nih.gov/pmc/articles/PMC1176254/.

Lærke, H. N., & Hedemann, M. S. (2012). The digestive system of the pig. In K. E. Bach Knudsen, N. J. Kjeldsen, H. D. Poulsen, & B. B. Jensen (Eds.), *Nutritional physiology of pigs – Online publication*. Foulum: Videncenter for Svineproduktion.

Li, H., Zhu, Y., Jiao, A., Zhao, J., Chen, X., Wei, B., … Tian, Y. (2013). Impact of α-amylase combined with hydrochloric acid hydrolysis on structure and digestion of waxy rice starch. *International Journal of Biological Macromolecules, 55*, 276–281. https://doi.org/10.1016/j.ijbiomac.2013.01.021

Lin, H. C., Kim, B. H., Elashoff, J. D., Doty, J. E., Gu, Y. G., & Meyer, J. H. (1992). Gastric emptying of solid food is most potently inhibited by carbohydrate in the canine distal ileum. *Gastroenterology, 102*(3), 793–801. https://doi.org/10.1016/0016-5085(92)90160-z

Martens, B. M. J., Bruininx, E. M. A. M., Gerrits, W. J. J., & Schols, H. A. (2020). The importance of amylase action in the porcine stomach to starch digestion kinetics. *Animal Feed Science and Technology, 267*, Article 114546. https://doi.org/10.1016/j.anifeedsci.2020.114546

Mennah-Govela, Y. A., Swackhamer, C., & Bornhorst, G. M. (2021). Gastric secretion rate and protein concentration impact intragastric pH and protein hydrolysis during dynamic in vitro gastric digestion. *Food Hydrocolloids for Health, 1*, Article 100027. https://doi.org/10.1016/j.fhfh.2021.100027

Miller, G. L. (1959). Use of dinitrosalicylic acid reagent for determination of reducing sugar. *Analytical Chemistry, 31*(3), 426–428. https://doi.org/10.1021/ac60147a030

Motoi, L., Morgenstern, M. P., Hedderley, D. I., Wilson, A. J., & Balita, S. (2013). Bolus moisture content of solid foods during mastication. *Journal of Texture Studies, 44*(468–479).

Nadia, J., Bronlund, J., Singh, H., Singh, R. P., & Bornhorst, G. M. (2021). Structural breakdown of starch-based foods during gastric digestion and its link to glycemic response: In vivo and in vitro considerations. *Comprehensive Reviews in Food Science and Food Safety, 20*(3), 2660–2698. https://doi.org/10.1111/1541-4337.12749

Nadia, J., Bronlund, J. E., Singh, H., Singh, R. P., & Bornhorst, G. M. (2022). Contribution of the proximal and distal gastric phases to the breakdown of cooked starch-rich solid foods during static in vitro gastric digestion. *Food Research International, 157*, Article 111270. https://doi.org/10.1016/j.foodres.2022.111270

Nadia, J., Olenskyj, A. G., Stroebinger, N., Hodgkinson, S. M., Estevez, T. G., Subramanian, P., … Bornhorst, G. M. (2021). Tracking physical breakdown of rice- and wheat-based foods with varying structures during gastric digestion and its influence on gastric emptying in a growing pig model. *Food & Function, 12*, 4349–4372.

Nau, F., Le Feunteun, S., Le Gouar, Y., Henry, G., Pasco, M., Guérin-Dubiard, C., … Dupont, D. (2022). Spatial-temporal mapping of the intra-gastric pepsin concentration and proteolysis in pigs fed egg white gels. *Food Chemistry, 389*, Article 133132. https://doi.org/10.1016/j.foodchem.2022.133132

Nau, F., Nyemb-Diop, K., Lechevalier, V., Floury, J., Serrière, C., Stroebinger, N., … Rutherfurd, S. M. (2019). Spatial-temporal changes in pH, structure and rheology of the gastric chyme in pigs as influenced by egg white gel properties. *Food Chemistry, 280*, 210–220. https://doi.org/10.1016/j.foodchem.2018.12.042

Ramadoss, B. R., Gangola, M. P., Agasimani, S., Jaiswal, S., Venkatesan, T., Sundaram, G. R., & Chibbar, R. N. (2019). Starch granule size and amylopectin chain length influence starch in vitro enzymatic digestibility in selected rice mutants with similar amylose concentration. *Journal of Food Science and Technology, 56*(1), 391–400. https://doi.org/10.1007/s13197-018-3500-8

Rosenblum, J. L., Irwin, C. L., & Alpers, D. H. (1988). Starch and glucose oligosaccharides protect salivary-type amylase activity at acid pH. *American Journal of Physiology, 254*(5 Pt 1), G775–G780. https://doi.org/10.1152/ajpgi.1988.254.5.G775

Salelles, L., Floury, J., & Le Feunteun, S. (2021). Pepsin activity as a function of pH and digestion time on caseins and egg white proteins under static in vitro conditions. *Food & Function, 12*(24), 12468–12478. https://doi.org/10.1039/D1FO02453A

Sangpring, Y., Fukuoka, M., & Ratanasumawong, S. (2015). The effect of sodium chloride on microstructure, water migration, and texture of rice noodle. *LWT – Food Science and Technology, 64*(2), 1107–1113. https://doi.org/10.1016/j.lwt.2015.07.035

Shewry, P. R. (2008). Improving the nutritional quality of cereals by conventional and novel approaches. In B. R. Hamaker (Ed.), *Technology of Functional Cereal Products* (pp. 159–183). Woodhead Publishing.

Siegel, J. A., Urbain, J. L., Adler, L. P., Charkes, N. D., Maurer, A. H., Krevsky, B., … Malmud, L. S. (1988). Biphasic nature of gastric emptying. *Gut, 29*(1), 85–89. https://doi.org/10.1136/gut.29.1.85

Tamura, M., Singh, J., Kaur, L., & Ogawa, Y. (2016). Impact of structural characteristics on starch digestibility of cooked rice. *Food Chemistry, 191*, 91–97. https://doi.org/10.1016/j.foodchem.2015.04.019

Weinstein, D. H., deRijke, S., Chow, C. C., Foruraghi, L., Zhao, X., Wright, E. C., … Wank, S. A. (2013). A new method for determining gastric acid output using a wireless pH-sensing capsule. *Alimentary Pharmacology & Therapeutics, 37*(12), 1198–1209. https://doi.org/10.1111/apt.12325

Woolnough, J. W., Bird, A. R., Monro, J. A., & Brennan, C. S. (2010). The effect of a brief salivary α-amylase exposure during chewing on subsequent in vitro starch digestion curve profiles. *International Journal of Molecular Sciences, 11*(8), 2780–2790. https://doi.org/10.3390/ijms11082780

Wu, P., Deng, R., Wu, X., Wang, Y., Dong, Z., Dhital, S., & Chen, X. D. (2017). In vitro gastric digestion of cooked white and brown rice using a dynamic rat stomach model. *Food Chemistry, 237*, 1065–1072. https://doi.org/10.1016/j.foodchem.2017.05.081

Zheng, Z., Stanley, R., Gidley, M. J., & Dhital, S. (2016). Structural properties and digestion of green banana flour as a functional ingredient in pasta. *Food & Function, 7*, 771. https://doi.org/10.1039/c5fo01156f

Zou, W., Sissons, M., Gidley, M. J., Gilbert, R. G., & Warren, F. J. (2015). Combined techniques for characterising pasta structure reveals how the gluten network slows enzymic digestion rate. *Food Chemistry, 188*, 559–568. https://doi.org/10.1016/j.foodchem.2015.05.032